



Defining the key pharmacophore elements of PF-04620110: Discovery of a potent, orally-active, neutral DGAT-1 inhibitor



Robert L. Dow^{*}, Melissa P. Andrews, Jian-Cheng Li, E. Michael Gibbs, Angel Guzman-Perez, Jennifer L. LaPerle, Qifang Li, Dawn Mather, Michael J. Munchhof, Mark Niosi, Leena Patel, Christian Perreault, Susan Tapley, William J. Zavadoski

PharmaTherapeutics Research & Development, Pfizer Inc., 620 Memorial Drive, Cambridge, MA 02139, United States

ARTICLE INFO

Article history:

Received 24 April 2013

Revised 10 June 2013

Accepted 19 June 2013

Available online 1 July 2013

Keywords:

DGAT-1

Diabetes

Obesity

Passive permeability

Carboxylic acid bioisotere

Polar surface area

ABSTRACT

DGAT-1 is an enzyme that catalyzes the final step in triglyceride synthesis. mRNA knockout experiments in rodent models suggest that inhibitors of this enzyme could be of value in the treatment of obesity and type II diabetes. The carboxylic acid-based DGAT-1 inhibitor **1** was advanced to clinical trials for the treatment of type 2 diabetes, despite of the low passive permeability of **1**. Because of questions relating to the potential attenuation of distribution and efficacy of a poorly permeable agent, efforts were initiated to identify compounds with improved permeability. Replacement of the acid moiety in **1** with an oxadiazole led to the discovery of **52**, which possesses substantially improved passive permeability. The resulting pharmacodynamic profile of this neutral DGAT-1 inhibitor was found to be similar to **1** at comparable plasma exposures.

© 2013 Elsevier Ltd. All rights reserved.

1. Introduction

Obesity and type 2 diabetes have been on a dramatic rise in Westernized countries over the last few decades, resulting in substantial societal burdens. The increased prevalence of these conditions is largely driven by a net imbalance between energy intake and expenditure. This in turn results in a net increase in fat disposition resulting from excess storage of triglycerides. The resulting increases in triglyceride stores in peripheral tissues, especially skeletal muscle, have been implicated in the development of insulin resistance¹ and the constellation of lipotoxic disorders associated with metabolic syndrome X.² Intracellular concentrations of lipids in muscle have been shown to be tightly, negatively correlated with insulin-stimulated glucose disposal in healthy males.³ This relationship is also found in humans with impaired glucose tolerance and type 2 diabetes.⁴ An additional line of evidence supporting the lipotoxicity hypothesis is the metabolic state of individuals suffering from the genetic disorders leading to lipodystrophy.⁵ Lipodystrophy is characterized by the absence of fat tissue, however, these individuals have excessive accumulation of lipids in metabolic tissues such as skeletal muscle and the liver. This aberrant distribution of lipids leads to an extreme

insulin-resistant state. In animal models of lipodystrophy, treatment with the adipose regulatory hormone leptin reduces intracellular lipid levels in skeletal muscle and other tissues, leading to improved insulin sensitivity.^{6,7} Given this critical role of lipid burden, oral therapies that have the potential to reverse this state hold significant potential in the treatment of type 2 diabetes, obesity and metabolic syndrome X.

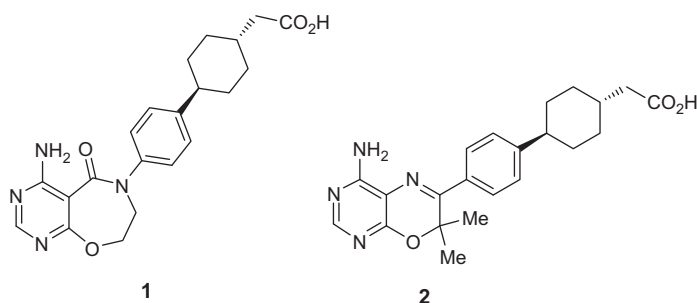
The enzymes involved in lipid biosynthesis pathways have attracted considerable interest as potential targets for disruption of aberrant lipid accumulation and its resulting impact on a range of disease states.^{8,9} Triglyceride biosynthesis and the resulting lipid burden placed on tissues are largely controlled by two major pathways in humans. The monoacylglyceride pathway is typically operative in tissues where dietary monoacylglycerides are reesterified, such as small intestine, liver and adipose.¹⁰ Fatty acids that enter this pathway come from dietary absorption or via de novo fatty acid synthesis from acetyl CoA, via a series of enzyme-catalyzed homology reactions. The second pathway, found in most cell types, is the glycerol phosphate pathway which sequentially adds two fatty acyl chains to glycerol-3-phosphate generating a phosphatidic acid intermediate that is subsequently converted to triglycerides.¹¹ Both of these pathways converge at intermediate diacylglycerols which are then converted to triglycerides through acylation by a fatty acid acyl-CoA, catalyzed by acyl-CoA:diacylglycerol acyltransferases (DGAT). This family of enzymes is

^{*} Corresponding author. Tel.: +1 (617) 551 3254; fax: +1 (845) 474 3821.

E-mail address: robert.l.dow@pfizer.com (R.L. Dow).

composed of DGAT-1 and DGAT-2, which while they carry out the same biotransformation, arise from divergent gene families.^{12–14} Consistent with the lipotoxicity hypothesis, mice lacking DGAT-1 (DGAT-1^{-/-}) are resistant to diet-induced obesity and have increased insulin sensitivity and energy expenditure.^{15,16} In addition, transplantation of white adipose tissue from these mice into the wild-type strain confers the enhanced metabolic profile observed in the DGAT-1 knockout mice.¹⁷ These studies have spurred research efforts to determine whether selective, small molecule inhibitors of DGAT-1 can produce the same improved metabolic profile observed in the DGAT-1^{-/-} animals.

Several research groups have disclosed potent and selective DGAT-1 inhibitors from several chemically-distinct series.¹⁸ Pre-clinical studies with these compounds have confirmed that small molecule DGAT-1 inhibitors can elicit metabolic outcomes comparable to those observed in DGAT-1^{-/-} mice.^{19–21} We have recently disclosed an orally-active, novel DGAT-1 inhibitor PF-04620110 (**1**) which was advanced to human clinical trials for the treatment of type 2 diabetes.²¹ This pyrimidooxazepinone-based series arose from specific design criteria aimed at eliminating the potential photochemical and reactive metabolite risks associated with the pyrimidinoxazine-based DGAT-1 inhibitor **2**.²² As compound **1** advanced into human clinical studies there were questions as to whether the poor passive permeability associated with agent would result in limited distribution into key *in vivo* compartments, potentially leading to a reduced efficacy maximum. This report details the discovery of neutral, potent and orally-active DGAT-1 inhibitors with high passive permeabilities and their resulting efficacy in preclinical rodent models. Analysis of the key pharmacophore elements of **1** will also be discussed as part of a broader structure–activity-relationship (SAR) analysis.

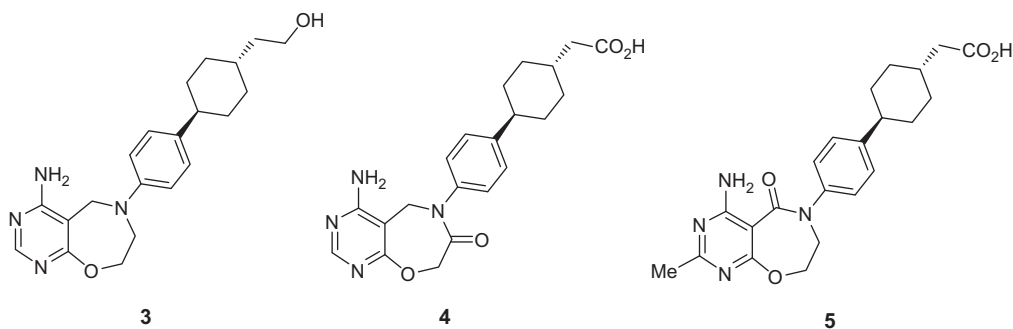


2. Results and discussion

As previously reported,²¹ the bicyclic core of **1** arose from analyses of alternative cores that retained what were assumed to be the key pharmacophore elements of **2** and the spatial orientation of these in three-dimensional space. Incorporation of the fused, seven-membered lactam moiety in **1** properly orients the cyclohexylacetic acid sidechain relative to **2** (Fig. 1). In addition, it eliminates the conjugated imine-based bicyclic present in **2**, which is likely

responsible for the photochemical instability associated with this lead. While our design resulted in a potent DGAT-1 inhibitor, with a pharmacokinetic/safety profile supporting its advancement to human clinical trials, there were a number of unanswered SAR questions relating to this novel chemotype. The combination of limited bicyclic core SAR disclosed around **2**²² and the inherent chemical differences between the two core structures, led us to pursue a systematic investigation of the key pharmacophore elements present in **1**.

While the in-plane orientation of the phenylcyclohexyl sidechain relative to the heterobicyclic cores of **1** and **2** (Fig. 1) suggested this to be a necessary requirement for potent DGAT-1 inhibition, alternative bicyclic cores that led to alternative spatial arrangements of these two pharmacophore elements were evaluated prior to further optimization of **1**. An additional goal was to improve on its low passive permeability (apparent passive permeability (P_{app}) = 1 mm 10⁻⁶ cm/s) associated with **1**. This property became the focus of our back-up effort since there was a concern that this low passive permeability might limit exposure to key target tissues *in vivo*. Computational models suggested that conversion of the lactam functionality in **1** to the corresponding bicyclic amine-based core could lead to a substantial increase in passive permeability (P_{app} = 7 × 10⁻⁶ cm/s).²³ Toward this end, global reduction of **1** afforded amine **3**. Modeling of the predicted low energy conformation of **3** (Fig. 1) suggested a significantly altered relationship between the core and sidechain relative to **1**. This modification led to a loss in DGAT-1 potency of >110-fold relative to **1** (Table 1). It is important to note that the loss in potency of **3** is not driven by reduction of the carboxylic acid functionality, given that a propyl alcohol analog of **1** is a potent inhibitor of DGAT-1 (unpublished data). An alternative lactam motif evaluated was



the regioisomeric lactam **4**. Modeling of this lactam suggested its low energy conformation would be similar to amine **3**, while retaining a neutral bicyclic core (Fig. 1). The lack of DGAT-1 inhibitory activity associated with **4** was consistent with the hypothesis that an in-plane relationship between the bicyclic core and phenylcyclohexyl sidechain found in **1** was critical. These results led to a focusing of efforts on analogs containing the pyrimidooxazepinone core present in **1**, with a goal of improving passive permeability.

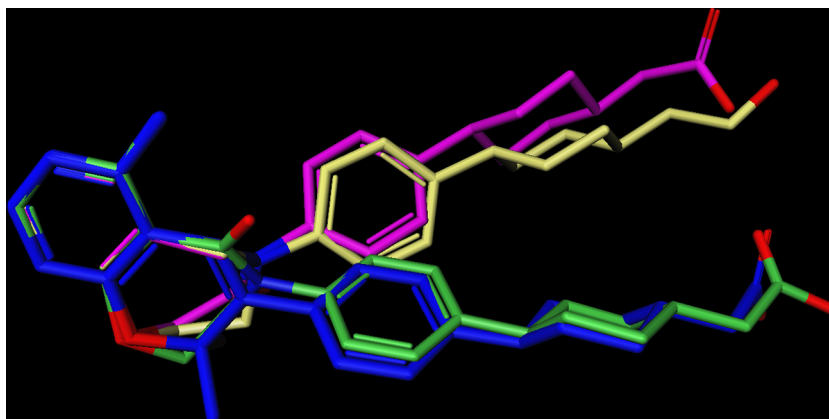
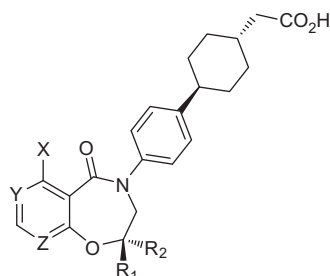


Figure 1. Overlay of crystal structure of **1** (green),²¹ minimized conformations of **2** (blue), **3** (yellow) and **4** (cyan).

Table 1

In vitro profiles of bicyclic core modifications of **1**



| | X | Y | Z | R ₁ ,R ₂ | hDGAT-1 IC ₅₀ ^a (nM) | TG synthesis IC ₅₀ ^b (nM) | HLM CL _{app} (mL/min/kg) | PSA |
|-----------|------------------|----|----|--------------------------------|--|---|-----------------------------------|-----|
| 1 | NH ₂ | N | N | H,H | 19 | 8 | <8 | 119 |
| 3 | | | | | 2960 | 1380 | 11 | 84 |
| 4 | | | | | >3000 | — | — | 119 |
| 5 | | | | | 59 | 44 | <8 | 119 |
| 6 | OH | N | N | H,H | >3000 | — | — | 113 |
| 7 | OMe | N | N | H,H | >3000 | — | — | 102 |
| 8 | NHMe | N | N | H,H | >3000 | — | — | 96 |
| 9 | NMe ₂ | N | N | H,H | >3000 | — | — | 105 |
| 10 | NH ₂ | N | CH | H,H | 1200 | — | — | 107 |
| 11 | NH ₂ | CH | N | H,H | 23 | 99 | 8.4 | 107 |
| 12 | NH ₂ | N | N | Me,Me | 146 | 32 | — | 119 |
| 13 | NH ₂ | N | N | H,Me | 625 | — | — | 119 |
| 14 | NH ₂ | N | N | Me,H | 19 | 8 | — | 119 |

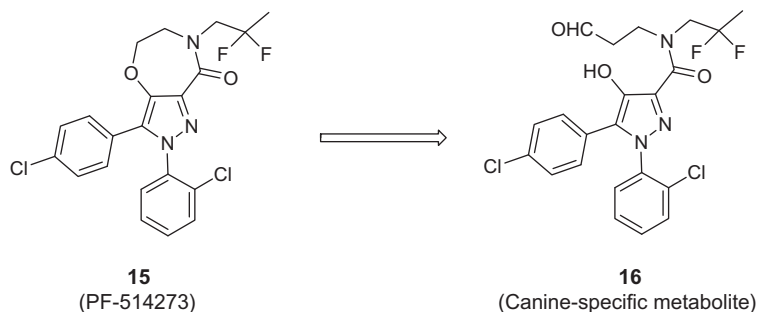
^a Average of ≥ 2 determinations run in triplicate.

^b Inhibition of triglyceride synthesis determined in HT-29 cells. Average of ≥ 2 determinations run in triplicate.

As part of a program to explore the key binding interactions between the core of **1** and DGAT-1 a systematic analysis of the aminopyrimidine subunit was initiated. A potential approach to improving passive permeability within this series would be to increase lipophilicity via incorporation of substituents in the 3-position of the pyrimidine ring. Towards this end a 3-methyl analog **5** was prepared and shown to be a potent inhibitor of DGAT-1 activity and triglyceride synthesis in HT-29 cells (Table 1). While low projected oxidative clearance was observed for this analog, the reduction in potency relative to **1** suggested that further efforts based on modification of the 3-position were unlikely to provide an improved balance of potency, permeability and microsomal stability. An alternative approach to improving permeability was to alter the amino group of **1** by replacement with less polar isosteric replacements or masking as a secondary/tertiary amine, which would result in reduced polar surface area (PSA). The corresponding hydroxy (**6**) or methoxy (**7**) analogs were devoid of DGAT-1 inhibitory activity. Conversion of the primary amine in **1** into the *N*-methyl (**8**) or *N,N*-dimethylamines (**9**) also led to a loss of activity.

These results demonstrate that the 4-amino substituent is critical for DGAT-1 inhibition. With a reduced PSA relative to **1**, the regioisomeric aminopyridines were prepared to determine if they offered an advantage. 2-Aminopyridine **10** had substantially reduced potency, though the 4-amino analog **11** was determined to have an IC₅₀ value of 23 nM against hDGAT-1 and inhibited triglyceride synthesis with an IC₅₀ value of 99 nM. While **11** exhibited a projected clearance profile comparable to **1**, its passive permeability ($P_{app} = 1 \times 10^{-6}$ cm/s) is not improved relative to the lead.

The structural core of **1** is similar to that in the cannabinoid receptor-1 receptor antagonist **15**,²⁴ which showed a substantial erosion of the therapeutic index in canine safety studies. Based on mechanism work it was hypothesized that formation of **16** was responsible for the observed toxicology (Scheme 1). Based on the structural overlap between **15** and **1** a two-pronged strategy to address this potential reactive metabolite issue was pursued. The first of these was a design approach based on steric blocking of the ether bearing carbon in **1** was pursued. If tolerated from a potency standpoint, incorporation of lipophilicity at this position



Scheme 1. Canine-specific metabolism of CB1-receptor antagonist PF-514273 (**15**).

would also have the potential to improve passive permeability. Substituents in this position would roughly overlap space occupied by the methyl groups on the quaternary carbon of **2**. The direct homolog **12** was less active than the **1**, however, preparation of the homochiral monomethyl derivatives revealed that each of these methyl groups was having a differential impact on DGAT-1 inhibitory activity. *S*-Isomer **13** had substantially reduced activity ($IC_{50} = 625$ nM), while its enantiomer **13** was equipotent to **1**. These results are consistent with the good overlap of the methyl group of **13** with the *pro-R* methyl of **2** while the methyl of **12** occupies novel space, likely resulting in a negative steric interaction with DGAT-1.

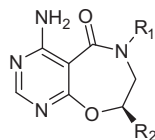
Monomethyl derivative **14** would be expected to dramatically reduce the potential for metabolic activation of the substituted carbon center, as well as any metabolic activation leading to a much less reactive keto-metabolite. In parallel to this design effort, a more detailed evaluation of the metabolic fate of **1** in human microsomal preparations was initiated. Acid **1** is very stable in human liver microsomes, with 93% of parent remaining after 1 h. Of the portion that is turned over there was no evidence of the putative aldehyde metabolite being formed based on trapping experiments with methoxymethylamine. This result gave us confidence in advancing **1** to human clinical studies.

With the above studies providing confidence that the pyrimidopyridinone core of **1** represented a highly optimized scaffold, attention turned to expanding the SAR for the phenylcyclohexylacetic acid sidechain. With **1** possessing a lipophilic carboxylic acid, it is reasonable to propose a binding site overlap with that occupied by the acyl CoA substrate in DGAT-1. However, kinetic analysis of inhibition of hDGAT-1 utilizing decanoyl CoA as the acyl donor revealed **1** to be a noncompetitive inhibitor with respect to this substrate ($R^2 = 0.98$). As for efforts on the bicyclic

core, a key goal was to drive designs into physicochemical space that would be predicted to lead to improved passive permeability. In order to gain an understanding of the minimum pharmacophore required to maintain potency in this system a series of truncated analogs of **1** were prepared. Both the parent bicyclic heterocycle **17** and *N*-methyl derivative **18** exhibited weak inhibition at 30 μ M (Table 2). Reestablishment of the *N*-aryl motif afforded substantial improvements in DGAT-1 inhibitory activity, with 4-alkyl functionalized analogs **19** and **20** possessing ligand efficiencies modestly improved relative to **1**.²⁶ Attempts to incorporate ionizable/polar functionality in the vicinity of the aryl ring (**21**) resulted in loss of DGAT-1 inhibitory activity. In order to understand whether general lipophilicity in this region of the inhibitor structure was sufficient for potency, a series of *N*-cycloalkyl analogs were evaluated. Cyclopentyl derivative **22** was found to have a reduced potency and ligand efficiency relative to neutral *N*-aryl analogs. For a more direct comparison the aromatic ring saturated analogs of **20** were prepared. The more active *N*-4-*t*-butylcyclohexyl isomer **24** was 20-fold less active than the corresponding aryl homolog. These results support a conclusion that the *N*-aryl motif present in **1** is optimal for DGAT-1 inhibitory activity.

In anticipation of an approach based on modification of the cyclohexylacetic acid subunit of **1** as a means of improving permeability, a set of analogs were prepared to map out the optimum display of the acidic functionality. Homologated acids **25** and **26** were found to be equipotent to **1**, although they had substantially reduced whole cell activities (Table 3). Tetrazole **27** was also a potent inhibitor of DGAT-1 but was right-shifted around 10-fold in the cell assay, due to poor permeability ($P_{app} < 0.1 \times 10^{-6}$ cm/s) resulting from increased PSA. These results led us to retain the core structure present in **1** in efforts to optimize permeability. From the very

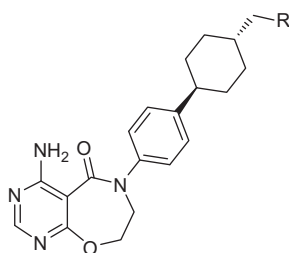
Table 2
In vitro profiles of truncated analogs **17–24**



| | R ₁ | R ₂ | hDGAT-1 IC ₅₀ ^a (nM) | TG synthesis IC ₅₀ ^b (nM) | LE ²⁵ | Permeability ²⁷ ($\times 10^{-6}$ cm/s) |
|-----------|--|----------------|--|---|------------------|---|
| 1 | | | 19 | 8 | 0.38 | 1 |
| 17 | H | H | 20% inhibition @ 30 μ M | — | — | — |
| 18 | Me | H | 36% inhibition @ 30 μ M | 25% inhibition @ 30 μ M | — | — |
| 19 | 4-Methylphenyl | H | 2210 | 681 | 0.41 | 33 |
| 20 | 4- <i>t</i> -Butylphenyl | H | 134 | 43 | 0.43 | 28 |
| 21 | 4-Carboxyphenyl | Me | 36% inhibition @ 30 μ M | 14% inhibition @ 30 μ M | — | — |
| 22 | Cyclopentyl | H | 92,100 | 9% inhibition @ 30 μ M | 0.32 | — |
| 23 | <i>cis</i> -4- <i>t</i> -Butylcyclohexyl | H | 27% inhibition @ 3 μ M | — | — | — |
| 24 | <i>trans</i> -4- <i>t</i> -Butylcyclohexyl | H | 2950 | — | 0.34 | — |

^a Average of ≥ 2 determinations run in triplicate.

^b Inhibition of triglyceride synthesis determined in HT-29 cells. Average of ≥ 2 determinations run in triplicate.

Table 3In vitro profiles of carboxylic acid replacements **25–38**

| | R | hDGAT-1 IC ₅₀ ^a (nM) | TG synthesis IC ₅₀ ^b (nM) | HLM CL _{app} (mL/min/kg) | PSA | Permeability ²⁷ (×10 ⁻⁶ cm/s) |
|-----------|---|--|---|-----------------------------------|-----|---|
| 1 | | 19 | 8 | <8 | 119 | 1 |
| 25 | | 31 | 131 | <8 | 119 | 4 |
| 26 | | 26 | 421 | <8 | 139 | <0.1 |
| 27 | | 76 | 774 | <8 | 136 | <0.1 |
| 28 | | 34 | — | — | 108 | 17 |
| 29 | | 32 | 34 | <8 | 124 | 4 |
| 30 | | 94 | — | <8 | 110 | 13 |
| 31 | | 64 | 13 | 39 | 110 | 22 |
| 32 | | 85 | 68 | <8 | 131 | 4 |
| 33 | | 45 | 110 | 15 | 102 | 24 |
| 34 | | 148 | 55 | <8 | 122 | 2 |
| 35 | | 94 | 60 | <8 | 111 | 11 |
| 36 | | 170 | 180 | 9 | 122 | 2 |
| 37 | | 50 | 66 | 107 | 111 | 22 |
| 38 | | 249 | 79 | <8 | 122 | — |

^a Average of ≥2 determinations run in triplicate.^b Inhibition of triglyceride synthesis determined in HT-29 cells. Average of ≥2 determinations run in triplicate.

Table 4
Rat pharmacokinetic profiles of key DGAT-1 inhibitors

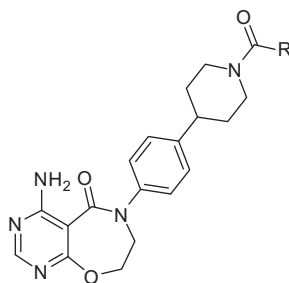
| | CL _p ^a (mL/min/kg) | V _{dss} ^a (L/kg) | C _{max} ^{b,c} (ng/mL) | AUC ^{b,c} (ng h/mL) | T _{1/2} (h) | %F |
|-----------|---|---|--|---------------------------------|-------------------------|-----|
| 1 | 6.7 | 1.8 | 225 | 565 | 7.3 | 100 |
| 29 | 11.7 | 1.6 | 273 | 810 | 4.3 | 88 |
| 35 | 17 | 1.2 | 425 | 838 | 2.0 | 77 |
| 49 | 8.4 | 2.0 | 174 | 801 | 3.1 | 85 |
| 50 | 7.2 | 1.3 | 171 | 1260 | 2.6 | 100 |
| 52 | 5.3 | 1.2 | 118 | 727 | 2.7 | 53 |

^a Intravenous dose of 1 mg/kg.^b Oral dose of 5 mg/kg dosed in 0.5% methylcellulose.^c Free drug concentrations.

early stages of investigations on **1**, the potent DGAT-1 inhibitory activity of neutral analogs such as methyl ester **28** and primary amide **29** demonstrated that an acidic functionality in the cyclohexylphenyl pharmacophore was not obligate for activity. Because **29** had improved passive permeability relative to **1** it was advanced to a rat pharmacokinetics. Though it had low/no detectable turnover in rat liver microsomes, **29** did have moderate clearance in the rat (Table 4). This enhanced turnover in vivo was consistent with the observation that **29** was unstable in plasma, presumably through conversion to **1** by plasma amidases/esterases.

To more fully explore the opportunity in this chemical space a series of compounds in which the carboxylic acid was replaced

with neutral moieties were pursued. A number of design criteria were employed in selection of targets, including calculated properties cutoffs for polar surface area (PSA <140), molecular weight (<500), predictive models of human microsomal clearance (<30 mL/min/kg) and passive permeability ($P_{app} > 5 \times 10^{-6}$ cm/s). Based on the excellent DGAT-1 inhibitory profile of primary amide **29**, a library of substituted amides was pursued. The primary goals for this set of compounds were to improve passive permeability relative to **1**, while also increasing in vivo half-life relative to **29**. Representative examples detailed in Table 3 (**30–38**) show that a range of secondary/tertiary amides with or without polar functionalities retain good to excellent levels of DGAT-1 enzyme and cell inhibitory activities. While introduction of modest lipophilicity (**31/33**) resulted in good passive permeability, there was an associated increase in oxidative clearance. Attempts to rebalance these two properties through incorporation of additional polarity was challenging given the high PSA starting point of the core structure. Incorporation of hydroxyl (**32/34/38**) or amide (**36**) functionalities led to enhanced microsomal stability, but decreased permeability and DGAT-1 potency. These results led us to focus efforts on amides with a PSA value intermediate between **33** and **34**, such as the morpholine and 4-methoxypiperidine amides, **35** and **37**. While the latter of these had high human microsomal clearance, **35** had a good balance of DGAT-1 activity, low clearance and good permeability. Rat pharmacokinetic analysis revealed this amide to have a half-life reduced relative to **1** and primary amide **29**. During

Table 5
In vitro profiles of *N*-acylpiperidines

| | R | hDGAT-1 IC ₅₀ ^a (nM) | TG synthesis IC ₅₀ ^b (nM) | HLM CL _{app} (mL/min/kg) | PSA | Permeability ²⁷ ($\times 10^{-6}$ cm/s) |
|-----------|------------------|--|---|-----------------------------------|-----|---|
| 39 | Methyl | 194 | 609 | <8 | 102 | 5 |
| 40 | <i>i</i> -Propyl | 174 | 601 | 11 | 102 | 16 |
| 41 | | 274 | 393 | – | 111 | 6 |
| 42 | | 85 | 514 | 41 | 102 | 21 |
| 43 | | 215 | 470 | <8 | 111 | 3 |
| 44 | | 113 | 574 | <8 | 122 | 1 |
| 45 | | 7 | 6750 | <8 | 141 | – |
| 46 | | 88 | 276 | <8 | 102 | 19 |
| 47 | | 79 | 1310 | 13 | 128 | 14 |
| 48 | | 174 | 830 | 12 | 128 | 16 |

^a Average of ≥ 2 determinations run in triplicate.^b Inhibition of triglyceride synthesis determined in HT-29 cells. Average of ≥ 2 determinations run in triplicate.

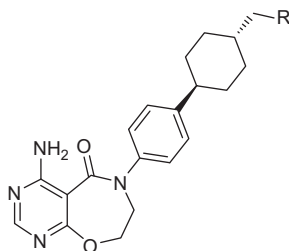
the course of this work both **29** and **35** were found to be positive in an in vitro micronucleus assay performed in the absence of metabolic activation. Based on these results efforts were shifted away from this series of amides.

In parallel with the above efforts, a library of amides in which the cyclohexylacetic acid moiety was replaced with a *N*-acylpiperazine were evaluated. Data for representative members of this library are detailed in Table 5. Compounds possessing small *N*-acyl substituents (e.g., **39–41**) had modest DGAT-1 inhibitory activity. Attempts to increase potency through the incorporation of more lipophilic substituents, such as in **42**, led to modest improvements in potency, but were accompanied by significant metabolic instability. Attenuating this lipophilicity through addition of polarity (**43** and **44**) were successful in reducing clearance potential (HLM <8 mL/min/kg), but resulted in poor passive permeability. A set of five-membered heterocycle-based amides were included in the initial library and of these oxadiazole **45** was identified as a potent inhibitor of DGAT-1 ($IC_{50} = 7$ nM). While this analog was 10-fold more potent than benzoyl derivative **46**, it suffered from a ~ 1000 -fold disconnect with respect to inhibition of triglyceride synthesis in HT-29 cells. This poor cellular activity was likely the result of poor cellular penetration driven by the high PSA of **46**.

Based on their predicted improved PSA and passive permeability a series of related oxazole and isoxazoles were prepared. While this approach did restore high passive permeability (e.g., **47** and **48**), all of these analogs had reduced potency and microsomal stability. These results suggest that it would be very difficult to generate a balanced pharmacology/ADME profile within this series.

Given the excellent in vitro pharmacology profiles of methyl ester **28** and primary amide **29** efforts were reengaged on neutral analogs of these leads, with a focus on non-amide replacements for the carboxylic acid functionality of **1**. Acetonitrile **49** was found to have a good balance of DGAT-1 inhibitory activity, microsomal stability and passive permeability (Table 6). Incorporation of a tertiary alcohol (**50**) is also well tolerated in terms of suppression of DGAT-1 activity, microsomal clearance and passive permeability. Though not neutral under physiological conditions, it is worth noting that the corresponding tertiary basic amine **51** retains good DGAT-1 potency, however, it suffers from poor passive permeability. Both **49** and **50** were evaluated in rat pharmacokinetic analyses and based on the relative profiles, the latter was advanced to a rat safety evaluation. In-life and clinical pathology analyses of Sprague-Dawley rats treated for four days with oral doses (5, 50 and 500 mg/kg) of **50** revealed a number of side effects at the mid

Table 6
In vitro profiles of neutral analogs of **1**



| | R | hDGAT-1 IC_{50} (nM) ^a | TG Synthesis IC_{50} (nM) ^b | HLM CL_{app} (mL/min/kg) | PSA | Permeability ²⁷ ($\times 10^{-6}$ cm/sec) |
|-----------|---|-------------------------------------|--|----------------------------|-----|---|
| 49 | | 64 | 41 | <8 | 105 | 27 |
| 50 | | 25 | 54 | <8 | 102 | 23 |
| 51 | | 40 | 70 | 12 | 107 | 2 |
| 52 | | 60 | 23 | <8 | 120 | 39 |
| 53 | | 210 | — | <8 | 120 | 12 |
| 54 | | 185 | — | <8 | 107 | 11 |
| 55 | | 391 | 253 | <8 | 123 | 6 |
| 56 | | 312 | — | <8 | 112 | 0.6 |
| 57 | | 37 | 70 | 82 | 120 | 22 |

^a Average of ≥ 2 determinations run in triplicate.

^b Inhibition of triglyceride synthesis determined in HT-29 cells. Average of ≥ 2 determinations run in triplicate.

Table 7
In vitro safety profile of **52**

| Endpoint | Result |
|-------------------------------|---------------------------------|
| hACAT-1 inhibition | IC ₅₀ >10 μM |
| hDGAT-2 inhibition | IC ₅₀ >30 μM |
| Broad ligand/enzyme profiling | IC ₅₀ >10 μM for All |
| hERG inhibition | 23% Inhibition @ 30 μM |
| Ames assay | Negative |
| In vitro micronucleus | Negative |

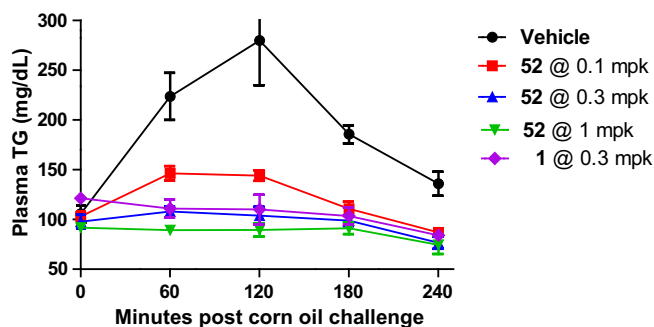


Figure 2. Acute plasma triglyceride lowering effects of **52** in C57BL/6 mice.

and high doses. These included skin turgor, reductions in body weight, increases in serum cholesterol and decreased T4 hormone levels. These results led us to consider other options for neutral replacements of the carboxylic acid moiety of **1**.

Given the well established ability of azoles to serve as bioisosteric replacements for amides and esters, a series of five-membered heterocycle-based analogs were pursued.²⁸ 1,2,4-Oxadiazole **52** was found to be a potent inhibitor of DGAT-1 and cellular triglyceride synthesis. Its balanced physicochemical properties (LogD = 2.3, PSA = 120) resulted in an excellent ADME profile with low microsomal clearance (<8 mL/min/kg) and high passive permeability (39×10^{-6} cm/s). Alternative oxadiazole, thiadiazole and triazole motifs (**53–56**) were found to have both reduced DGAT-1 inhibitory activities and passive permeabilities. Given the profile of oxadiazole **52** the corresponding homologated analog **57** was evaluated. While incorporation of an additional methylene unit had no significant impact on DGAT-1 inhibitory activity relative to **52**, it was found to have substantially reduced metabolic stability (HLM CL_{app} = 82 mL/min/kg). From this set of neutral heterocyclic-based analogs, oxadiazole **52** was selected for further pharmacokinetic, safety and efficacy profiling. Pharmacokinetic profiling in rat revealed **52** to have low clearance (5.3 mL/min/kg) and moderate oral bioavailability of 53% (Fig. 4). These data

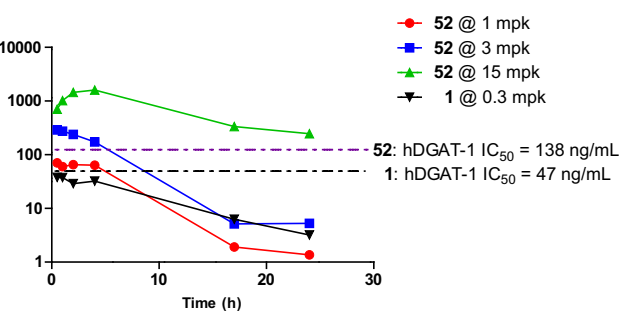
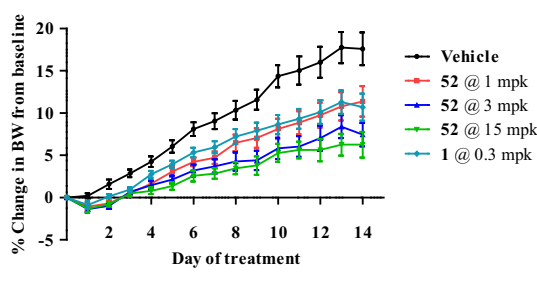


Figure 3. Body weight gain and food intake changes induced by chronic treatment of db/db mice with **52**.

in combination with the low turnover in human microsomes predict an attractive pharmacokinetic profile in humans.

Compound **52** was very selective versus the closet DGAT-1 enzymatic family members hACAT-1 and hDGAT-2 (Fig. 7). The risk of off-target pharmacology presenting a safety issue for **52** appeared to be minimal based on selectivity indices of >150-fold for a panel of 140 human receptors and channels. Negative results in Ames and in vitro micronucleus analyses suggested low genetic toxicology risk for this compound. No detectable inhibition against a panel of human cytochrome P-450 isoforms indicated low probability of drug–drug interactions in the human clinical setting. Patch clamp analysis of the potential hERG liability **52** revealed an IC₅₀ >30 μM. Based on this in vitro safety profile, **52** was advanced to a four day rat safety evaluation at doses of 5, 50 and 500 mg/kg (po). No significant clinical signs, changes in body/liver weights or histology/hematological endpoints were observed at all doses. The only findings were slight elevations in total cholesterol (1.5-fold), total triiodothyronine levels (1.3-fold, with no impact on thyroxine or thyroid-stimulating hormone) and liver enzymes (ALT, 1.5-fold) at 500 mg/kg. Based on this encouraging safety profile, compound **52** was advanced to acute and chronic in vivo efficacy evaluations (Table 7).

The pharmacodynamic potential of compound **52** was initially evaluated in an oral triglyceride tolerance test. C57BL/6 mice were treated with vehicle, 0.1, 0.3 or 1 mg/kg of **52** 30 min prior to dosing with a corn oil bolus. Plasma triglyceride (TG) levels were monitored every hour over the course of the 4 h test period. Compound **52** inhibited the increase in plasma TG levels in a dose dependent manner, with complete suppression of TG excursion at a dose of 0.3 mg/kg (Fig. 2). These results compared favorably with what is seen for the lead clinical candidate **1**, which exhibits a comparable potency in this assay.

Compound **52** was advanced to a chronic efficacy study in db/db mice maintained on a high fat diet. Animals were dosed with 0.5% methylcellulose vehicle, compound **52** (1, 3 or 15 mg/kg, po, Q.D.)

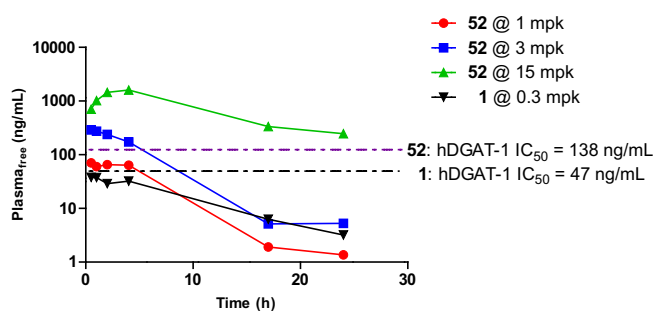


Figure 4. Day 14 free plasma exposures of **52** in mouse db/db chronic study.

or **1** (0.3 mg/kg) for 14 days. Over the course of the study body weight and food intake were measured daily for each animal ($n = 8/\text{dose}$). Plasma endpoints, TG and non-esterified fatty acids (NEFA) were measured on days 0, 7 and 14. On day 14, liver tissue levels of TG and glycogen were evaluated. Separate satellite groups ($n = 4/\text{dose}$) was utilized for drug exposure measurements. Over the course of the 14 day treatment, compound **52** produced a dose-responsive reduction in body weight (Fig. 3). This effect on body weight was sustained throughout the course of the study, with no rebound in weight gain observed. While there is an initial relative reduction in food intake (FI) relative to controls in the first few days of the study, FI rebounded at the mid-point in the study to then

parallel the vehicle treatment group. This suggests that the weight loss observed in these animals was not driven entirely by the reduction in FI. The magnitude of weight loss at 1 mg/kg of **52** is approximately equivalent to that observed for **1** at a comparable dose (0.3 mg/kg). Free drug plasma exposures generated in satellite animals are plotted in Figure 4 (murine plasma_{fu} = 0.09 and 0.35 for **52** and **1**, respectively). At the highest dose of **52**, plasma free drug exposures were greater than the hDGAT-1 IC₅₀ (murine data not generated) over the duration of the study. At lower doses, exposures were maintained at or near the IC₅₀ for several hours during the course of a 24 h period. The disconnect between IC₅₀ coverage and observed efficacy for the lowest dose of **52** and **1**, could be

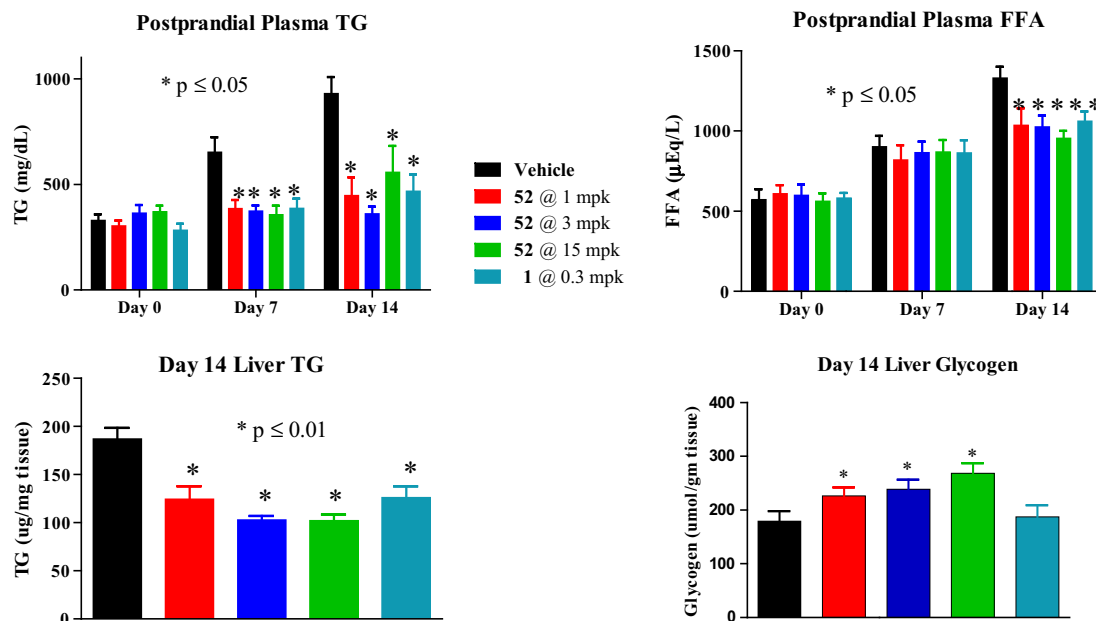
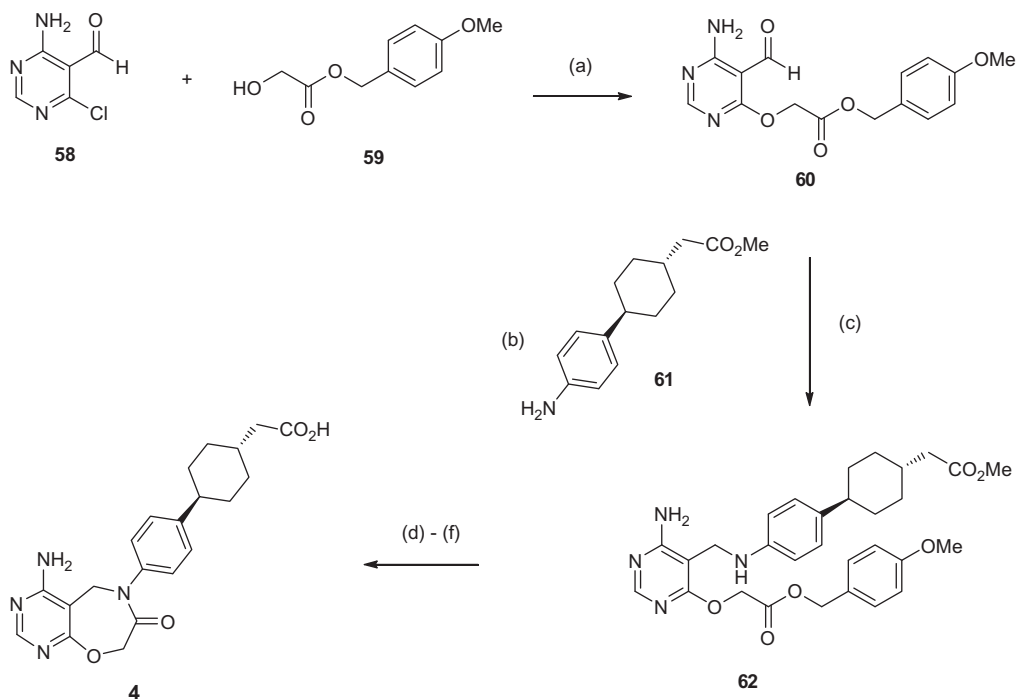
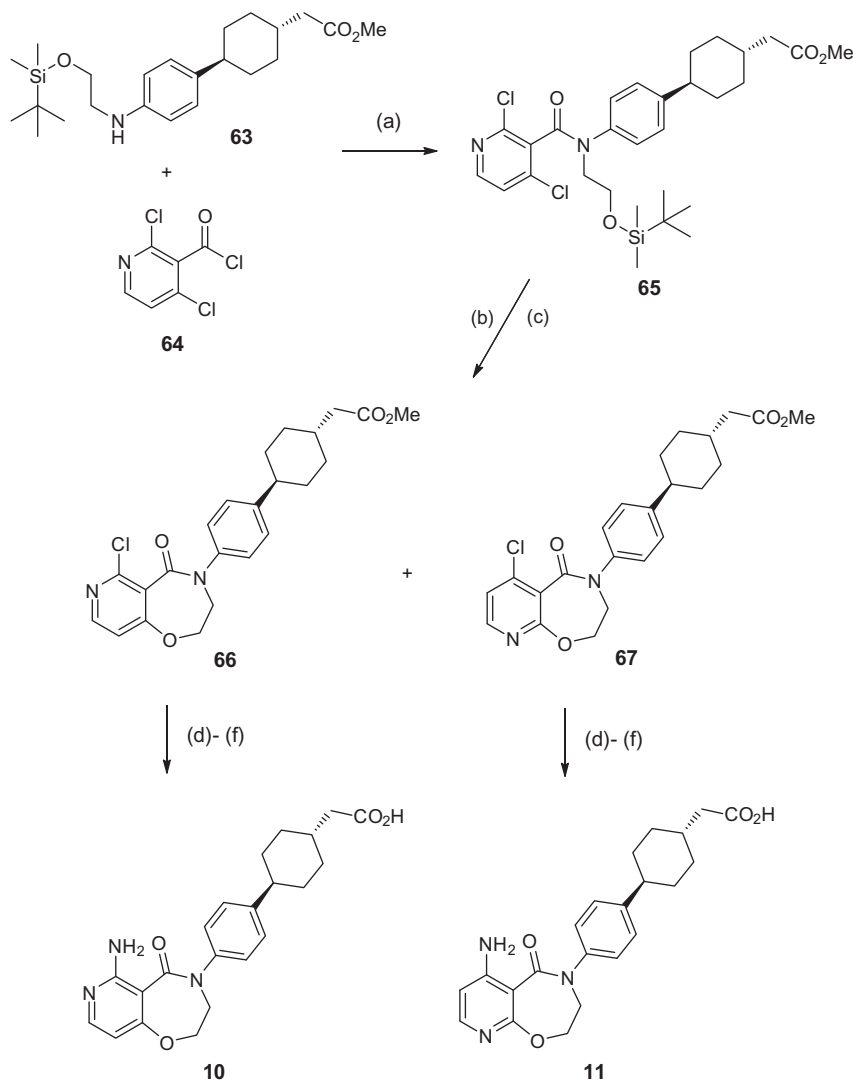


Figure 5. Triglyceride and free fatty acid changes induced by chronic treatment of db/db mice with **52**.



Scheme 2. Synthesis of pyrimidooxazepinone **3**. Reagents and conditions: (a) NaH, THF; (b) 1,2-dichloroethane, 60 °C; (c) sodium triacetoxyborohydride, 1,2-dichloroethane; (d) trifluoroacetic acid, 1,2-dichloroethane; (e) 1,1-carbonyldiimidazole, DMAP, DMF, 60 °C; (f) lithium hydroxide, 1,4-dioxane, H₂O.



Scheme 3. Syntheses of pyridooxazepinones **10** and **11**. Reagents and conditions: (a) Et_3N , THF, 0°C ; (b) MeOH, aq HCl I, 25°C ; (c) Cs_2CO_3 , acetonitrile, reflux; (d) 4-methoxybenzylamine, Et_3N , DMA, sealed tube, 140°C ; (e) TFA, 50°C ; (f) LiOH, H_2O , *p*-dioxane.

the result of difference in species pharmacology or efficacy being driven in part by DGAT-1 inhibition in the liver/intestine, where drug concentrations are likely elevated relative to plasma.

Postprandial plasma triglycerides were significantly reduced relative to vehicle control at days 7 and 14 for all doses of **52** and **1** (Fig. 5). There was no dose response to this effect since plasma TG levels were essentially restored to basal levels at all doses of **52**. As expected with treatment with a high-fat diet the control mice had increased levels of plasma free fatty acids (FFA) over the course of the study. With DGAT-1 being responsible for not only synthesis, but also hydrolysis of TG, it was not clear what impact inhibiting this enzyme would have on FFA in this study. While no significant changes in plasma FFA levels for the treatment groups were observed on day 7, by the end of the study levels were substantially reduced at all doses of DGAT-1 inhibitor treatment relative to the control animals. Similar effects were also observed for liver TG levels after 14 days of treatment with **52**. This reduction in liver TG content is consistent with what is observed in DGAT1^{-/-} mice.²⁹ In high fat fed rodent models an inverse relationship between increased liver TG and reduced glycogen levels has been described as a hallmark of the insulin resistant state.³⁰ In the current study, day 14 liver glycogen levels were increased relative to control animals in a dose-responsive manner (Fig. 5). This profile of increased liver glycogen and reduced TG levels

observed for **52** is consistent with DGAT-1 inhibition leading to an improvement in insulin resistance.

3. Chemistry

Preparation of analogs **5**, **12–25** were accomplished utilizing the general procedures previously described for **1**.²¹ Given the relatively chemical inert nature of the 4-aminopyrimidooxazepinone core, a wide range of chemistries could be carried out on advanced intermediates.

The regioisomeric 4-aminopyrimidooxazepinone **3** was prepared starting with condensation of chloroaldehyde **58** with the sodium salt of α -hydroxyester **59** (Scheme 2). Reduction of the imine prepared from **60** and aniline **61** afforded benzylic amine **62**. Selective deprotection of the benzyl ester protecting group followed by CDI-mediated lactamization and hydrolysis of the methyl ester afforded **3**.

Preparation of the regioisomeric pyridooxazepinones **10** and **11** was accomplished utilizing the synthetic sequence depicted in Scheme 3. Amide coupling of **63**²¹ and acid chloride **64** afforded amide **65**. Removal of the alcohol protecting group, followed by base catalyzed cyclization afforded a 1:2.4 mixture of regioisomeric chloropyridines **66** and **67**, which were separated by chromatography.

The primary amine functionality was incorporated via condensation with 4-methoxybenzylamine and deprotection with trifluoroacetic acid. Base-catalyzed hydrolysis afforded acids **10** and **11**.

Syntheses of the neutral heterocycle-based analogs of **1** are depicted in Scheme 4. Condensation of the acid chloride of **1** with *N*-hydroxyacetamide afforded **68** which was thermally cyclized to

afford oxadiazole **52**. Regioisomeric oxadiazole **53** was generated by dehydrative cyclization of bis-acetylated hydrazine **69**. This intermediate was also utilized to prepare the corresponding thiadiazole **54**. Condensation of the acid chloride of **1** with acetamidrazone, followed by thermal cyclization provided triazole analog **55**. The corresponding *N*-methyl homolog **56** was prepared via condensation of thioamide **71** with acetyl hydrazide.

4. Conclusion

During preclinical evaluation of the prototypical DGAT-1 inhibitor **1** there were concerns around potential restriction of tissue distribution due to its associated low passive permeability, which in turn could limit efficacy. This led to initiation of a back-up program focused on the identification of analogs with enhanced passive permeability, while retaining the positive features of **1**. The high polar surface area associated with this carboxylic acid-based structure limited the options available for tuning the properties to achieve acceptable passive permeability. Extensive SAR studies led to the identification of the neutral, oxadiazole **52** which is a potent hDGAT-1 inhibitor, with a balanced ADME profile. Off-target pharmacology and in vivo toleration analyses suggest that this compound is a selective DGAT-1 inhibitor, with an encouraging safety profile. Pharmacokinetic and pharmacodynamic evaluations revealed this neutral compound possessed comparable maximal efficacy relative to **1**, suggesting that the polar nature of **1** did not inhibit exposure to key efficacy tissues in preclinical models. However, if the rodent PK/PD models do not translate into low doses in humans, there is the risk that the maximal absorbable dose of **1** will likely be capped due to its poor permeability. Thus, the enhanced permeability of **52** will likely allow a higher dosing paradigm in humans and that will allow for greater flexibility in addressing the potential of DGAT-1 inhibition in treating obesity and diabetes.

5. Experimental

5.1. Chemistry

NMR spectra were recorded on a Varian Unity™ 400 or 500 (Varian Inc., Palo Alto, CA) at room temperature at 400 and 500 MHz ¹H, respectively. Chemical shifts are expressed in parts per million (δ) relative to residual solvent as an internal reference. The peak shapes are denoted as follows: s, singlet; d, doublet; t, triplet; q, quartet; m, multiplet; br s, broad singlet; v br s, very broad singlet; br m, broad multiplet; 2s, two singlets.

Mass spectrometry analysis was also obtained by reversed phase HPLC gradient method for chromatographic separation. Molecular weight identification was recorded by positive and negative electrospray ionization (ESI) scan modes. A Waters/Micro-mass ESI/MS model ZMD or LCZ mass spectrometer equipped with Gilson 215 liquid handling system and HP 1100 DAD was used to carry out the experiments.

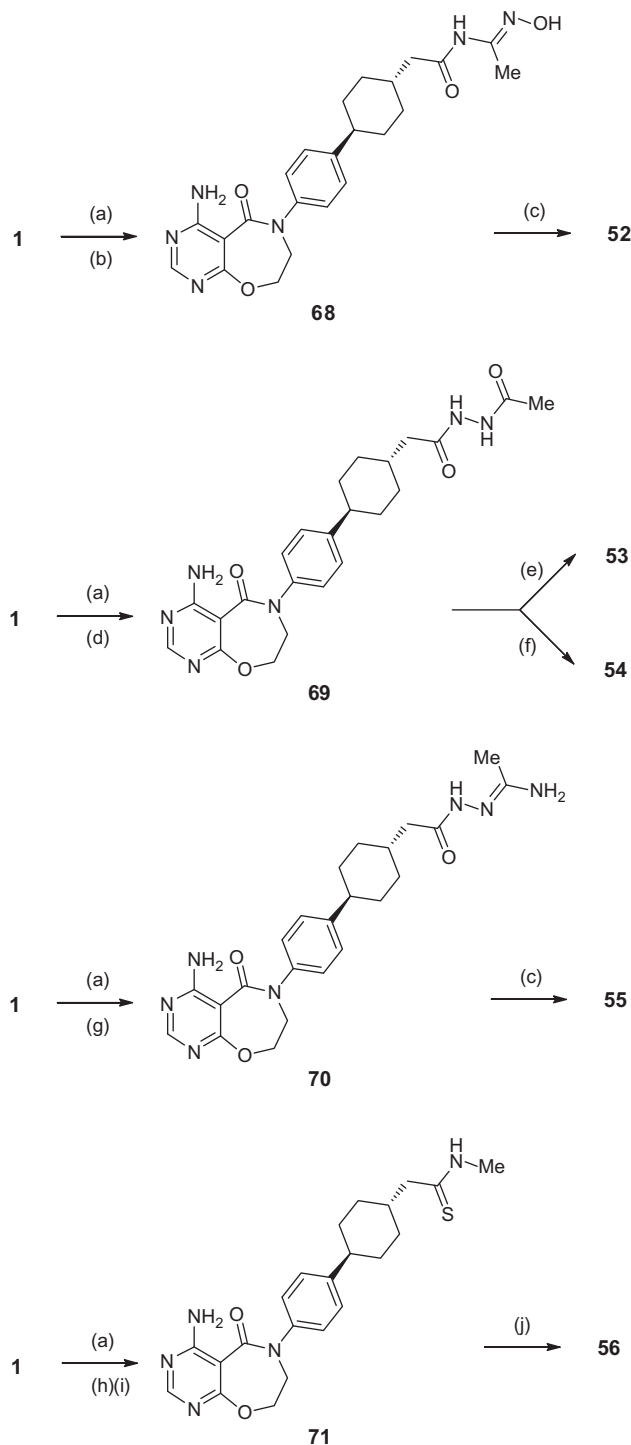
Purity determinations on all test compounds were determined HPLC analysis. All compounds for which biochemical data is reported are of ≥95% purity.

Silica gel column chromatography was performed with Bio-tage™ columns (ISC, Inc., Shelton, CT) under low nitrogen pressure.

PF-04620110 was initially synthesized at Pfizer, but is now commercially available through Sigma Aldrich.

5.1.1. 2-{*trans*-4-[4-(4-Amino-7,8-dihydropyrimido[5,4-*f*][1,4]oxazepin-6(5*H*)-yl)phenyl]cyclohexyl}ethanol (**3**)

To a stirred, cooled (0 °C) solution of **28** (103 mg, 0.25 mmol) in tetrahydrofuran (20 mL) was added a 1 M tetrahydrofuran solution of lithium aluminum hydride (0.50 mL, 0.5 mmol). After 3 h, the



Scheme 4. Synthesis of heterocycles **52**–**56**. Reagents and conditions: (a) oxalyl chloride, dichloroethane; (b) hydroxyacetamide, *p*-dioxane; (c) DMF, sealed tube, 120 °C; (d) acetyl hydrazide, *p*-dioxane; (e) triphenylphosphine, iodine, triethylamine, dichloromethane; (f) Lawesson's reagent, tetrahydrofuran, sealed tube, 120 °C; (g) acetamidrazone hydrochloride, tetrahydrofuran, triethylamine; (h) methylamine hydrochloride, triethylamine, dichloromethane; (i) Lawesson's reagent, tetrahydrofuran, reflux; (j) mercury oxide, acetyl hydrazide, tetrahydrofuran, microwave.

reaction was quenched by sequential addition of water (20 μ L), 15% aqueous sodium hydroxide (20 μ L) and then additional water (60 μ L) and the resulting slurry was stirred for 1 h at room temperature. Filtration through a pad of Celite[®], washing with 10% isopropanol/dichloromethane and concentration in vacuo afforded a sticky white solid. Chromatography on silica gel (4 g column, 1–8% methanol/chloroform) afforded the title compound as a white solid, 4 mg. ¹H NMR (400 MHz, methanol-*d*₄) δ 7.90 (s, 1H), 6.96 (d, 2H), 6.58 (d, 2H), 4.52 (dd, 2H), 4.40 (s, 2H), 3.77 (dd, 2H), 3.55 (t, 2H), 2.30 (br t, 1H), 1.84–1.73 (m, 4H), 1.44–1.00 (m, 7H). LCMS (ESI) *m/z*: 383.4 (M+H).

5.1.2. {*trans*-4-[4-(4-Amino-7-oxo-7,8-dihydropyrimido[5,4-*f*][1,4]oxazepin-6(5*H*)-yl)phenyl]cyclohexyl}acetic acid (4)

To a stirred solution of **59** (2.44 g, 12.4 mmol) in tetrahydrofuran (42 mL) was added sodium hydride (0.6 g of 60% in oil, 14.9 mmol). After 15 min, **58** (1.96 g, 12.4 mmol) was added and the resulting yellow slurry was stirred for 17 h. The reaction mixture was quenched with aqueous ammonium chloride, tetrahydrofuran was removed in vacuo and the resulting slurry extracted with ethyl acetate. The organic phase was dried over sodium sulfate and concentrated in vacuo to afford **60** as a yellow solid, 3.71 g. ¹H NMR (400 MHz, chloroform-*d*) δ 10.28 (s, 1H), 8.62 (br s, 1H), 8.15 (s, 1H), 7.07–7.40 (m, 2H), 6.64–7.00 (m, 2H), 5.81 (br s, 1H), 5.13 (s, 2H), 4.85–5.04 (m, 2H), 3.78 (s, 3H). LCMS (ESI) *m/z*: 318.3 (M+H).

A stirred solution of **60** (3.58 g, 5.60 mmol) and **61** (1.81 g, 7.32 mmol) in 1,2-dichloroethane (56 mL) was heated at 60 °C for 24 h. An additional portion of **61** (0.42 g) was added and heating was continued for 4 h and then allowed to cool to ambient temperature. The resulting solution was used as is in the next step.

The above solution was treated with sodium triacetoxyborohydride (3.16 g, 14.2 mmol). After 17 h, saturated aqueous ammonium chloride was added (10 mL), the organic layer was washed with water, dried over sodium sulfate and concentrated in vacuo to afford **62** as a white solid, 2.93 g. ¹H NMR (400 MHz, chloroform-*d*) δ 1.00–1.20 (m, 2H) 1.34–1.49 (m, 2H) 1.83 (d, *J* = 11.72 Hz, 5H) 2.21 (d, *J* = 6.64 Hz, 2H) 2.34 (t, *J* = 12.20 Hz, 1H) 3.46 (br s, 1H) 3.64 (s, 3H) 3.77 (s, 3H) 4.20 (d, *J* = 3.32 Hz, 2H) 4.87 (s, 2H) 5.10 (s, 2H) 5.37 (s, 2H) 6.65 (d, *J* = 8.40 Hz, 2H) 6.77–6.89 (m, 2H) 7.02 (d, *J* = 8.40 Hz, 2H) 7.13–7.29 (m, 2H) 8.09 (s, 1H). LCMS (ESI) *m/z*: 549.5 (M+H).

To a stirred solution of **62** (2.90 g, 5.29 mmol) in dichloromethane (5 mL) was added trifluoroacetic acid (1.22 g, 10.6 mmol). After 1 h, the solution was concentrated in vacuo, the residue was recrystallized from ethyl acetate/heptanes to afford an off-white solid, 2.40 g. ¹H NMR (400 MHz, DMSO-*d*₆) δ 0.89–1.11 (m, 2H) 1.18–1.40 (m, 2H) 1.52–1.78 (m, 5H) 2.16 (d, *J* = 6.83 Hz, 2H) 2.18–2.27 (m, 1H) 3.53 (s, 3H) 4.03 (s, 2H) 4.80 (s, 2H) 6.54 (d, *J* = 8.20 Hz, 2H) 6.61 (br s, 2H) 6.85 (d, *J* = 8.40 Hz, 2H) 7.94 (s, 1H). LCMS (ESI) *m/z*: 429.1 (M+H).

A solution of the solid obtained above (39 mg, 0.09 mmol), 1,1-carbonyldiimidazole (30 mg, 0.18 mmol) and 4-*N,N*-dimethylaminopyridine (0.1 mg, 0.001 mmol) in dimethylformamide (1 mL) was stirred at 60 °C for 24 h. The solution was diluted into ethyl acetate, washed with water, the organic layer dried over sodium sulfate and concentrated in vacuo. Chromatography of the residue on silica gel (0–10% methanol/dichloromethane, 4 g column) afforded an off-white solid, 7.7 mg. ¹H NMR (400 MHz, DMSO-*d*₆) δ 1.00–1.15 (m, 2H) 1.31–1.46 (m, 2H) 1.60–1.83 (m, 5H) 2.19 (d, *J* = 6.64 Hz, 2H) 2.34–2.43 (m, 1H) 3.54 (s, 3H) 4.80 (s, 2H) 4.96 (s, 2H) 6.84 (s, 2H) 7.06 (d, 2H) 7.20 (d, 2H) 7.93 (s, 1H). LCMS (ESI) *m/z*: 411.3 (M+H).

To a stirred solution of the above solid (5 mg, 0.01 mmol) 1,4-dioxane (0.1 mL) and water (0.025 mL) was added a 1 M solution of aqueous lithium hydroxide (0.036 mL). This solution was heated

at 50 °C for 1 h, cooled and acidified to pH ~3 with 1 M aqueous hydrogen chloride. 1,4-Dioxane was removed in vacuo and the aqueous mixture was extracted with 10% *i*-propanol/dichloromethane, the organic layer dried over sodium sulfate and concentrated in vacuo. Chromatography on silica gel (0–10% methanol/dichloromethane, 4 g column) afforded the title compound as an off-white solid, 3.3 mg. ¹H NMR (400 MHz, methanol-*d*₄) δ 1.17–1.25 (m, 2H) 1.43–1.61 (m, 2H) 1.76–2.00 (m, 5H) 2.21 (d, *J* = 6.83 Hz, 2H) 2.42–2.59 (m, 1H) 4.88 (s, 2H) 5.09 (s, 2H) 7.15 (d, *J* = 8.40 Hz, 2H) 7.27 (d, *J* = 8.40 Hz, 2H) 7.83 (s, 1H) 8.03 (s, 1H). LCMS (ESI) *m/z*: 397.1 (M+H).

5.1.3. {*trans*-4-[4-(4-Amino-2-methyl-5-oxo-7,8-dihydropyrimido[5,4-*f*][1,4]oxazepin-6(5*H*)-yl)phenyl]cyclohexyl}acetic acid (5)

Prepared in analogy to compound 1.²¹ ¹H NMR (400 MHz, chloroform-*d*) δ 8.25 (br s, 1H), 7.35 (d, 2H), 7.18 (d, 2H), 6.64 (br s, 1H), 4.70–4.64 (m, 2H), 4.03–3.96 (m, 2H), 2.50 (dd, 1H), 2.43 (s, 3H), 2.31–2.24 (m, 2H), 1.99–1.85 (m, 5H), 1.59–1.43 (m, 2H), 1.24–1.16 (m, 2H). LCMS (ESI) *m/z*: 411.4 (M+H).

5.1.4. {*trans*-4-[4-(4-Hydroxy-5-oxo-7,8-dihydropyrimido[5,4-*f*][1,4]oxazepin-6(5*H*)-yl)phenyl]cyclohexyl}acetic acid (6) / {*trans*-4-[4-(4-methoxy-5-oxo-7,8-dihydropyrimido[5,4-*f*][1,4]oxazepin-6(5*H*)-yl)phenyl]cyclohexyl}acetic acid (7)

A stirred solution of methyl (*trans*-4-[4-[[4,6-dichloropyrimidin-5-yl]carbonyl](2-hydroxyethyl)amino]phenyl)cyclohexyl acetate²¹ (5.69 g, 12.2 mmol) and potassium carbonate (5.06 g, 36.6 mmol) in methanol (24.4 mL) was heated at reflux for 2 h. After cooling, the methanol was removed in vacuo, the residue partitioned between ethyl acetate/water, the organic phase was dried over sodium sulfate and concentrated in vacuo to afford a white solid, 5.19 g. LCMS (ESI) *m/z*: 426.2 (M+H).

To a heated (50 °C), stirred solution of the above solid (1.50 g, 3.52 mmol) in *p*-dioxane (10 mL)/water (1 mL) was added an aqueous solution of lithium hydroxide (5 mL, 1 M). After 3 h, the reaction was cooled and concentrated in vacuo. The residue was suspended in water, acidified to pH ~3 with 1 N aqueous hydrochloric acid and stirred for 5 min. The solids were filtered and air dried. A 50 mg portion of these solids were purified by reverse phase HPLC (Phenominix[®] C18 30 \times 50 mm column, 15–100% acetonitrile/water (1% formic acid) gradient) to afford **6** (7.5 mg) and **7** (31 mg). Compound **6**: ¹H NMR (400 MHz, DMSO-*d*₆) δ 8.15 (s, 1H), 7.23 (AB q, 4H), 4.58 (t, 2H), 4.02 (t, 2), 2.50–2.42 (m, 1H), 2.13 (d, 2H), 1.85–1.64 (m, 5H), 1.53–1.40 (m, 2H), 1.18–1.03 (m, 2H). LCMS (ESI) *m/z*: 396.1 (M–H). Compound **7**: LCMS (ESI) *m/z*: 412.2 (M+H).

5.1.5. (*trans*-4-[4-[4-(Methylamino)-5-oxo-7,8-dihydropyrimido[5,4-*f*][1,4]oxazepin-6(5*H*)-yl]phenyl]cyclohexyl}acetic acid (8)

A solution of methyl {*trans*-4-[4-(4-chloro-5-oxo-7,8-dihydropyrimido[5,4-*f*][1,4]oxazepin-6(5*H*)-yl)phenyl]cyclohexyl} acetate²¹ (352 mg, 0.82 mmol) and a 2 M solution of methylamine in THF (1.5 mL, 3 mmol) were stirred at ambient temperature for 65 h. The solution was concentrated in vacuo to afford a white solid, 340 mg. LCMS (ESI) *m/z*: 425.2 (M+H).

A solution of the above solids and 1 M aqueous lithium hydroxide (2.5 mL, 2.5 mmol) in *p*-dioxane (5 mL) was heated at 50 °C for 1.5 h. The reaction mixture was cooled, concentrated in vacuo, the solids were suspended in water and the pH adjusted to ~3 with 6 N aqueous hydrochloric acid. The resulting solids were filtered and dried at 50 °C in a vacuum oven for 17 h to afford the title compound as an off-white solid, 314 mg. ¹H NMR (400 MHz, chloroform-*d*) δ 11.97 (br s, 1H), 8.61 (br s, 1H), 8.38 (s, 1H), 7.24 (d, 2H), 7.08 (d, 2H), 4.62 (dd, 2H), 3.97 (dd, 2H), 2.98 (s, 3H), 2.57–

2.43 (m, 1H), 2.29 (d, 2H), 1.97–1.82 (m, 5H), 1.67–1.43 (m, 2H), 1.24–1.10 (m, 2H). LCMS (ESI) *m/z*: 411.1 (M+H).

5.1.6. (*trans*-4-[4-[4-(Dimethylamino)-5-oxo-7,8-dihydropyrimido[5,4-*f*][1,4]oxazepin-6(5H)-yl]phenyl]cyclohexyl)acetic acid (9)

Prepared in analogy to compound **8**. ¹H NMR (400 MHz, DMSO-*d*₆) δ 12.00 (br s, 1H), 8.23 (s, 1H), 7.26 (s, 4H), 4.47 (dd, 2H), 4.10 (br s, 2H), 3.00 (s, 6H), 2.50–2.41 (m, 1H), 2.10 (d, 2H), 1.82–1.63 (m, 5H), 1.53–1.38 (m, 2H), 1.18–1.03 (m, 2H). LCMS (ESI) *m/z*: 425.2 (M+H).

5.1.7. (*trans*-4-[4-(6-Amino-5-oxo-2,3-dihydropyrido[3,4-*f*][1,4]oxazepin-4(5H)-yl)phenyl]cyclohexyl)acetic acid (10)

A stirred solution of 2-chloro-4-iodonicotinic acid (2.0 g, 7.0 mmol), one drop of dimethylformamide and thionyl chloride (4.36 g, 36.7 mmol) was heated at 65 °C for 17 h. After cooling, the reaction solution was azeotroped with toluene twice to afford **64** as a dark liquid.

To a stirred, cooled (0 °C) solution **63** (2.24 g, 5.52 mmol) and diisopropylethylamine (2.8 g, 3.8 mmol) in tetrahydrofuran (6 mL) was a solution of **64** (2.00 g, 10.0 mmol) in tetrahydrofuran (6 mL) dropwise over a 15-min period. The reaction was then allowed to stir at ambient temperature for 17 h, diluted into ethyl acetate, washed with water and saturated aqueous sodium bicarbonate. The organic layer was dried over sodium sulfate, concentrated in vacuo and chromatographed on silica gel (100 g column, 10–60% ethyl acetate/heptanes) to afford **65** as a red oil, 2.45 g. ¹H NMR (400 MHz, chloroform-*d*) δ 0.02 (s, 6H) 0.83 (s, 9H) 1.09 (t, *J* = 13.92 Hz, 2H) 1.29–1.43 (m, 2H) 1.72–1.89 (m, 5H) 2.21 (d, *J* = 6.65 Hz, 2H) 2.34 (t, *J* = 12.05 Hz, 1H) 3.65 (s, 3H) 3.84–3.92 (m, 2H) 3.95–4.03 (m, 2H) 6.99 (d, *J* = 8.31 Hz, 2H) 7.07 (d, *J* = 5.40 Hz, 1H) 7.27 (d, *J* = 8.31 Hz, 2H) 8.05 (d, *J* = 5.40 Hz, 1H). LCMS (ESI) *m/z*: 579.2 (M+H).

A solution of **65** (2.45 g, 4.23 mmol) in 3% concd HCl/methanol (17 mL) was stirred at ambient temperature for 1 h. The methanol was removed in vacuo, the residue diluted into ethyl acetate, washed with saturated aqueous sodium bicarbonate, water, dried over sodium sulfate and concentrated in vacuo to afford a dark red oil, 2.15 g. ¹H NMR (400 MHz, chloroform-*d*) δ 0.96–1.18 (m, 2H) 1.29–1.46 (m, 2H) 1.80 (dd, *J* = 22.22, 11.42 Hz, 5H) 2.21 (d, *J* = 6.65 Hz, 2H) 2.35 (t, *J* = 12.05 Hz, 1H) 3.65 (s, 3H) 3.82–3.96 (m, 2H) 4.00–4.11 (m, 2H) 7.03 (d, *J* = 8.31 Hz, 2H) 7.10 (d, *J* = 5.40 Hz, 1H) 7.29 (d, *J* = 8.72 Hz, 2H) 8.08 (d, *J* = 5.40 Hz, 1H). LCMS (ESI) *m/z*: 465.0 (M+H).

A slurry of the above oil (402 mg, 0.86 mmol) and cesium carbonate (1.13 g, 3.46 mmol) in acetonitrile (4.8 mL) was stirred at reflux for 20 h. The reaction mixture was cooled, diluted into ethyl acetate, washed with water, dried over sodium sulfate and concentrated in vacuo to afford an oil. Chromatography on silica gel (25 g column, 10–70% ethyl acetate/heptane) afforded **66** (67 mg) and **67** (162 mg) as white solids. Compound **66**: ¹H NMR (400 MHz, chloroform-*d*) δ 1.06–1.25 (m, 2H) 1.34–1.57 (m, 2H) 1.88 (d, *J* = 10.39 Hz, 5H) 2.24 (d, *J* = 5.40 Hz, 2H) 2.49 (t, *J* = 12.25 Hz, 1H) 3.67 (s, 3H) 3.89 (t, *J* = 4.78 Hz, 2H) 4.55 (t, *J* = 4.78 Hz, 2H) 7.15–7.44 (m, 5H) 8.29 (d, *J* = 7.06 Hz, 1H). LCMS (ESI) *m/z*: 429.0 (M+H). **67**: ¹H NMR (400 MHz, chloroform-*d*) δ 1.03–1.22 (m, 2H) 1.37–1.57 (m, 2H) 1.88 (d, *J* = 10.80 Hz, 5H) 2.25 (d, *J* = 6.65 Hz, 2H) 2.38–2.59 (m, 1H) 3.67 (s, 3H) 3.92 (t, *J* = 5.19 Hz, 2H) 4.49 (t, *J* = 5.19 Hz, 2H) 6.96 (d, *J* = 5.40 Hz, 1H) 7.17–7.40 (m, 4H) 8.36 (d, *J* = 5.40 Hz, 1H). LCMS (ESI) *m/z*: 429.0 (M+H).

A solution of **66** (89 mg, 0.21 mmol), 4-methoxybenzylamine (85 mg, 0.62 mmol) and triethylamine (105 mg, 1.0 mmol) in dimethylacetamide (2.3 mL) was heated at 140 °C in a sealed tube for 3 h. The cooled reaction solution was diluted into ethyl acetate, washed with water, dried over sodium sulfate and concentrated in

vacuo to afford an oil. Chromatography on silica gel (10 g column, 20–50% ethyl acetate) afforded a white solid, 90 mg. ¹H NMR (400 MHz, chloroform-*d*) δ 1.02–1.25 (m, 2H) 1.35–1.60 (m, 2H) 1.87 (d, *J* = 11.22 Hz, 5H) 2.24 (d, *J* = 6.65 Hz, 2H) 2.38–2.57 (m, 1H) 3.67 (s, 3H) 3.75 (s, 3H) 3.90 (t, *J* = 5.19 Hz, 2H) 4.44 (t, *J* = 5.19 Hz, 2H) 4.54 (d, *J* = 4.98 Hz, 2H) 6.27 (d, *J* = 5.40 Hz, 1H) 6.80 (d, *J* = 8.72 Hz, 2H) 7.15–7.35 (m, 6H) 8.12 (d, *J* = 5.82 Hz, 1H). LCMS (ESI) *m/z*: 530.0 (M+H).

A solution of the solid from the previous step (90 mg, 0.17 mmol) in trifluoroacetic acid (2.5 mL) was heated at 50 °C in a sealed tube for 3 h. The reaction solution was concentrated in vacuo, the residue diluted into ethyl acetate, washed with saturated aqueous sodium bicarbonate, dried over sodium sulfate and concentrated in vacuo to afford a white solid, 70 mg. ¹H NMR (400 MHz, chloroform-*d*) δ 1.07–1.23 (m, 2H) 1.42–1.57 (m, 2H) 1.78–1.97 (m, 5H) 2.25 (d, *J* = 7.06 Hz, 2H) 2.49 (t, *J* = 12.25 Hz, 1H) 3.67 (s, 3H) 3.91 (t, *J* = 5.19 Hz, 2H) 4.47 (t, *J* = 4.98 Hz, 2H) 6.33 (d, *J* = 5.82 Hz, 1H) 7.20–7.30 (m, 4H) 8.02 (d, *J* = 5.40 Hz, 1H). LCMS (ESI) *m/z*: 410.0 (M+H).

A solution of the solid from the previous step (50 mg, 0.12 mmol) and lithium hydroxide (8.8 mg, 0.34 mmol) in a solution of tetrahydrofuran/methanol/water (3:2:1, 3 mL) was stirred at ambient temperature for 20 h. The reaction was acidified to pH 4 with 1 N aqueous hydrochloric acid and the resulting solids were filtered and dried in vacuo to afford the title compound as a white powder, 5.8 mg. ¹H NMR (400 MHz, DMSO-*d*₆) δ 1.02–1.18 (m, 2H) 1.30–1.53 (m, 2H) 1.63–1.88 (m, 5H) 2.11 (d, *J* = 7.06 Hz, 2H) 2.38–2.55 (m, 1H) 3.85 (t, *J* = 5.19 Hz, 2H) 4.39 (t, *J* = 4.98 Hz, 2H) 6.27 (d, *J* = 5.40 Hz, 1H) 7.26 (s, 4H) 7.95 (d, *J* = 5.40 Hz, 1H). LCMS (ESI) *m/z*: 396.0 (M+H).

5.1.8. (*trans*-4-[4-(6-Amino-5-oxo-2,3-dihydropyrido[3,2-*f*][1,4]oxazepin-4(5H)-yl)phenyl]cyclohexyl)acetic acid (11)

Employing intermediate **67** the title compound was prepared in analogy to **10**. ¹H NMR (400 MHz, DMSO-*d*₆) δ 0.94–1.18 (m, 2H) 1.27–1.55 (m, 2H) 1.64–1.87 (m, 5H) 2.12 (d, *J* = 6.64 Hz, 2H) 2.36–2.55 (m, 1H) 4.07 (t, 2H) 4.70 (t, *J* = 5.19 Hz, 2H) 6.68 (d, *J* = 7.06 Hz, 1H) 7.29 (s, 4H) 7.86 (d, *J* = 6.64 Hz, 1H). LCMS (ESI) *m/z*: 396.0 (M+H).

5.1.9. (*trans*-4-[4-(4-Amino-8,8-dimethyl-5-oxo-7,8-dihydropyrimido[5,4-*f*][1,4]oxazepin-6(5H)-yl)phenyl]cyclohexyl)acetic acid (12)

Prepared in analogy to compound **1**.²¹ ¹H NMR (400 MHz, DMSO-*d*₆): δ 8.18 (s, 1H), 7.59 (br s, 1H) 7.20 (m, 4H), 3.79 (m, 2H), 2.42 (m, 1H), 2.08 (m, 2H), 1.78 (m, 4H), 1.67 (m, 1H), 1.43 (m, 2H), 1.24 (s, 6H), 1.66 1.05 (m, 2H). LCMS (ESI) *m/z*: 425.3 (M+H).

5.1.10. (*trans*-4-[4-[(8*S*)-4-Amino-8-methyl-5-oxo-7,8-dihydropyrimido[5,4-*f*][1,4]oxazepin-6(5H)-yl]phenyl]cyclohexyl)acetic acid (13)

Prepared in analogy to compound **1**.²¹ ¹H NMR (400 MHz, methanol-*d*₄): δ 8.19 (s, 1H), 7.33 (d, 2H), 7.24 (d, 2H), 5.04–4.94 (m, 1H), 3.92–3.87 (m, 2H), 2.58–2.44 (m, 1H), 2.25–2.18 (m, 2H), 1.93–1.86 (m, 5H), 1.60–1.46 (m, 2H), 1.35 (d, 3H), 1.28–1.10 (m, 2H). LCMS (ESI) *m/z*: 411.2 (M+H).

5.1.11. *trans*-4-[4-[(8*R*)-4-Amino-8-methyl-5-oxo-7,8-dihydropyrimido[5,4-*f*][1,4]oxazepin-6(5H)-yl]phenyl]cyclohexyl)acetic acid (14)

Prepared in analogy to compound **1**.²¹ ¹H NMR (400 MHz, methanol-*d*₄) δ 1.11–1.25 (m, 2H) 1.36 (d, *J* = 6.64 Hz, 3H) 1.53 (q, *J* = 12.88 Hz, 2H) 1.75–1.96 (m, 5H) 2.21 (d, *J* = 7.03 Hz, 2H) 2.46–2.58 (m, 1H) 3.80–3.96 (m, 2H) 4.92–5.03 (m, 1H) 7.25 (d, 2H) 7.31 (d, 2H) 8.17 (s, 1H). LCMS (ESI) *m/z*: 411.1(M+H).

Compounds **17–24** were prepared in analogy to **1**.²¹

5.1.12. 4-Amino-7,8-dihydropyrimido[5,4-f][1,4]oxazepin-5(6H)-one (17)

Prepared in analogy to compound **1**.²¹ ¹H NMR (400 MHz, DMSO-*d*₆) δ 9.08 (br s, 1H), 8.65 (br s, 1H), 8.35 (br s, 1H), 8.23 (s, 1H), 4.53 (m, 2H), 3.45 (m, 2H). LCMS (ESI) *m/z*: 181.4 (M+H).

5.1.13. 4-Amino-6-methyl-7,8-dihydropyrimido[5,4-f][1,4]oxazepin-5(6H)-one (18)

Prepared in analogy to **1**.²¹ ¹H NMR (400 MHz, methanol-*d*₄) δ 8.08 (s, 1H), 4.57–4.52 (m, 2H), 3.67–3.63 (m, 2H), 3.12 (s, 3H). LCMS (ESI) *m/z*: 195.3 (M+H).

5.1.14. 4-Amino-6-(4-methylphenyl)-7,8-dihydropyrimido[5,4-f][1,4]oxazepin-5(6H)-one (19)

Prepared in analogy to **1**.²¹ ¹H NMR (400 MHz, chloroform-*d*) δ 8.23 (s, 1H), 7.22 (d, 2H), 7.11 (d, 2H), 4.64–4.62 (m, 2H), 3.97–3.94 (m, 2H), 2.36 (s, 3H). LCMS (ESI) *m/z*: 271.3 (M+H).

5.1.15. 4-Amino-6-(4-*tert*-butylphenyl)-7,8-dihydropyrimido[5,4-f][1,4]oxazepin-5(6H)-one (20)

Prepared in analogy to **1**.²¹ ¹H NMR (400 MHz, methanol-*d*₄) δ 8.3 (s, 1H), 7.5 (d, 2H), 7.2 (d, 2H), 4.7 (t, 2H), 4.0 (t, 2H), 1.3 (s, 9H). LCMS (ESI) *m/z*: 313.5 (M+H).

5.1.16. 4-[(8*R*)-4-Amino-8-methyl-5-oxo-7,8-dihydropyrimido[5,4-f][1,4]oxazepin-6(5H)-yl]benzoic acid (21)

Prepared in analogy to **1**.²¹ ¹H NMR (400 MHz, methanol-*d*₄) δ 8.20 (s, 1H), 8.12–8.07 (m, 2H), 7.52–7.46 (m, 2H), 5.05–4.95 (m, 1H), 3.98 (d, 2H), 1.39 (d, 3H). LCMS (ESI) *m/z*: 315.3 (M+H).

5.1.17. 4-Amino-6-cyclopentyl-7,8-dihydropyrimido[5,4-f][1,4]oxazepin-5(6H)-one (22)

Prepared in analogy to **1**.²¹ ¹H NMR (400 MHz, methanol-*d*₄) δ 8.12 (s, 1H), 4.50–4.48 (m, 2H), 3.62–3.58 (m, 2H), 1.96–1.44 (m, 9H). LCMS (ESI) *m/z*: 249.3 (M+H).

5.1.18. 4-Amino-6-(*cis*-4-*tert*-butylcyclohexyl)-7,8-dihydropyrimido[5,4-f][1,4]oxazepin-5(6H)-one (23)

Prepared in analogy to **1**.²¹ ¹H NMR (400 MHz, chloroform-*d*) δ 8.25 (s, 1H), 4.78 (m, 1H), 4.49 (t, 2H), 3.353 (t, 2H), 1.88 (m, 4H), 1.27 (m, 4H), 1.00 (m, 1H), 0.86 (s, 9H). LCMS (ESI) *m/z*: 319.5 (M+H).

5.1.19. 4-Amino-6-(*trans*-4-*tert*-butylcyclohexyl)-7,8-dihydropyrimido[5,4-f][1,4]oxazepin-5(6H)-one (24)

Prepared in analogy to **1**.²¹ ¹H NMR (400 MHz, chloroform-*d*₃) δ 8.3 (s, 1H), 4.6 (m, 1H), 4.5 (t, 2H), 3.5 (t, 2H), 1.9 (m, 4H), 1.4–1.2 (m, 4H), 1 (m, 1H), 0.9 (s, 9H). LCMS (ESI) *m/z*: 319.5 (M+H).

5.1.20. 3-{*trans*-4-[4-(4-Amino-5-oxo-7,8-dihydropyrimido[5,4-f][1,4]oxazepin-6(5H)-yl)phenyl]cyclohexyl}propanoic acid (25)

Prepared in analogy to **1**.²¹ ¹H NMR (400 MHz, DMSO-*d*₆) δ 0.93–1.08 (m, 2H) 1.18–1.30 (m, 1H) 1.32–1.46 (m, 4H) 1.69–1.82 (m, 4H) 2.14–2.23 (m, 2H) 3.22–3.30 (m, 1H) 3.85–3.95 (m, 2H) 4.49–4.56 (m, 2H) 7.15–7.26 (m, 4H) 7.54 (s, 2H) 8.11 (s, 1H) 11.93 (s, 1H). LCMS (ESI) *m/z*: 411.1 (M+H).

5.1.21. 6-(4-(*trans*-4-(2*H*-Tetrazol-5-yl)methyl)cyclohexyl)phenyl)-4-amino-7,8-dihydropyrimido[5,4-f][1,4]oxazepin-5(6H)-one (27)

To a stirred, cooled (0 °C) solution of trimethylaluminum (2 M in toluene, 0.33 mL) were added trimethylsilylazide (38 mg, 0.33 mmol) and **49** (25 mg, 0.07 mmol). The reaction was heated at 80 °C for 40 h, cooled and concentrated in vacuo. The residue was chromatographed on silica gel (0–10% methanol/chloroform, 4 g column) to afford the title compound as a white solid, 2.8 mg.

¹H NMR (400 MHz, DMSO-*d*₆): δ 8.10 (s, 1H), 7.55 (br s, 2H), 7.29–7.13 (m, 4H), 4.57–4.45 (m, 2H), 3.95–3.85 (m, 2H), 2.76–2.62 (m, 2H), 2.50–2.31 (m, 1H), 1.80–1.62 (m, 5H), 1.45–1.25 (m, 2H), 1.28–0.96 (m, 2H). LCMS (ESI) *m/z*: 421.3 (M+H).

5.1.22. 4-Amino-6-{4-[*trans*-4-(2-oxo-2-pyrrolidin-1-ylethyl)cyclohexyl]phenyl}-7,8-dihydropyrimido[5,4-f][1,4]oxazepin-5(6H)-one (33)

A solution of **1** (12 mg, 0.03 mmol), pyrrolidine (5 mg, 0.08 mmol) and *O*-benzotriazole-*N,N,N',N'*-tetramethyl-uronium-hexafluoro-phosphate (12 mg, 0.04 mmol) in dimethylformamide (0.4 mL) was heated at 55 °C for 18 h. Chromatography on silica gel (4 g, 1–5% methanol/dichloromethane) afforded the title compound as a white solid, 7 mg. ¹H NMR (400 MHz, chloroform-*d*) δ 8.24 (s, 1H) 8.15 (br s, 1H) 7.10–7.35 (m, 4H) 5.63 (br s, 1H) 4.60–4.70 (m, 2H) 3.91–4.03 (m, 2H) 3.35–3.49 (m, 4H) 2.39–2.53 (m, 1H) 2.13–2.21 (m, 2H) 1.76–1.98 (m, 9H) 1.38–1.55 (m, 2H) 1.04–1.18 (m, 2H). LCMS (ESI) *m/z*: 450.4 (M+H).

The following amides were prepared in analogy to **33**.

5.1.23. *N*-{*trans*-4-[4-(4-Amino-5-oxo-7,8-dihydropyrimido[5,4-f][1,4]oxazepin-6(5H)-yl)phenyl]cyclohexyl}acetyl)-*N*-methylglycine (26)

¹H NMR (400 MHz, DMSO-*d*₆) δ 8.17 (s, 1H), 7.59 (br s, 2H), 7.28 (s, 4H), 4.58 (d, 2H), 3.96 (d, 2H), 3.33 (s, 3H), 3.00 (s, 2H), 2.50–2.43 (m, 1H), 2.24–2.10 (m, 2H), 1.87–1.69 (m, 5H), 1.50–1.40 (m, 2H), 1.18–1.03 (m, 2H). LCMS (ESI) *m/z*: 468.4 (M+H)

5.1.24. 2-*trans*-4-[4-(4-Amino-5-oxo-7,8-dihydropyrimido[5,4-f][1,4]oxazepin-6(5H)-yl)phenyl]cyclohexyl}acetamide (29)

¹H NMR (400 MHz, DMSO-*d*₆) δ 1.05 (br s, 2H) 1.26–1.50 (m, 2H) 1.59–1.71 (m, 1H) 1.75 (d, *J* = 11.32 Hz, 4H) 1.92 (d, *J* = 7.03 Hz, 2H) 2.34–2.54 (m, 1H) 3.91 (t, *J* = 4.49 Hz, 2H) 4.41–4.63 (m, 2H) 6.66 (br s, 1H) 7.13 (br s, 2H) 7.17–7.32 (m, 4H) 7.54 (s, 1H) 8.11 (s, 1H). LCMS (ESI) *m/z*: 396.3 (M+H).

5.1.25. 2-{*trans*-4-[4-(4-Amino-5-oxo-7,8-dihydropyrimido[5,4-f][1,4]oxazepin-6(5H)-yl)phenyl]cyclohexyl}-*N*-ethylacetamide (30)

¹H NMR (400 MHz, DMSO-*d*₆) δ 8.17 (s, 1H), 7.75 (br s, 1H), 7.57 (br s, 2H), 7.12 (s, 4H), 4.53 (dd, 2H), 3.90 (dd, 2H), 3.00 (q, 2H), 2.47–2.39 (m, 1H), 1.97–1.92 (m, 2H), 1.79–1.65 (m, 5H), 1.44–1.36 (m, 2H), 1.08–0.94 (m, 5H). LCMS (ESI) *m/z*: 424.5 (M+H).

5.1.26. 2-{*trans*-4-[4-(4-Amino-5-oxo-7,8-dihydropyrimido[5,4-f][1,4]oxazepin-6(5H)-yl)phenyl]cyclohexyl}-*N*-cyclopentylacetamide (31)

LCMS (ESI) *m/z*: 464.2 (M+H).

5.1.27. 2-{*trans*-4-[4-(4-Amino-5-oxo-7,8-dihydropyrimido[5,4-f][1,4]oxazepin-6(5H)-yl)phenyl]cyclohexyl}-*N*-[(1*R*)-1-(hydroxymethyl)-2-methylpropyl]acetamide (32)

LCMS (ESI) *m/z*: 482.1 (M+H).

5.1.28. 4-Amino-6-[4-(*trans*-4-{2-[(3*R*)-3-hydroxypyrrolidin-1-yl]-2-oxoethyl}cyclohexyl)phenyl]-7,8-dihydropyrimido[5,4-f][1,4]oxazepin-5(6H)-one (34)

LCMS (ESI) *m/z*: 466.1 (M+H).

5.1.29. 4-Amino-6-{4-[*trans*-4-(2-morpholin-4-yl-2-oxoethyl)cyclohexyl]phenyl}-7,8-dihydropyrimido[5,4-f][1,4]oxazepin-5(6H)-one (35)

¹H NMR (400 MHz, chloroform-*d*) δ 0.98–1.15 (m, 2H) 1.25–1.37 (m, 1H) 1.36–1.50 (m, 2H) 1.50–1.61 (m, 2H) 1.79–1.92 (m, 4H) 2.24–2.38 (m, 2H) 2.40–2.56 (m, 1H) 3.37–3.51 (m, 2H) 3.52–3.68 (m, 6H) 3.90–4.01 (m, 2H) 4.65 (dt, *J* = 4.98, 3.81 Hz, 2H).

2H) 5.63 (br s, 1H) 7.10–7.32 (m, 4H) 8.13 (s, 1H) 8.24 (s, 1H). LCMS (ESI) *m/z*: 480.5 (M+H).

5.1.30. 4-Amino-6-(4-{*trans*-4-[2-(4-methyl-3-oxopiperazin-1-yl)-2-oxoethyl]cyclohexyl}phenyl)-7,8-dihydropyrimido[5,4-*f*][1,4]oxazepin-5(6H)-one (36)

LCMS (ESI) *m/z*: 493 (M+H).

5.1.31. 4-Amino-6-(4-{*trans*-4-[2-(4-methoxypiperidin-1-yl)-2-oxoethyl]cyclohexyl}phenyl)-7,8-dihydropyrimido[5,4-*f*][1,4]oxazepin-5(6H)-one (37)

¹H NMR (400 MHz, chloroform-*d*) δ 8.23 (s, 1H) 8.14 (br s, 1H) 7.11–7.30 (m, 4H) 4.60–4.68 (m, 2H) 3.88–4.00 (m, 3H) 3.61–3.74 (m, 1H) 3.15–3.46 (m, 5H) 2.39–2.52 (m, 1H) 2.23 (dd, *J* = 6.64, 3.73 Hz, 2H) 1.76–1.96 (m, 8H) 1.39–1.60 (m, 5H) 1.03–1.17 (m, 2H). LCMS (ESI) *m/z*: 494.5 (M+H).

5.1.32. 4-Amino-6-(4-{*trans*-4-[2-(3-hydroxyazetididin-1-yl)-2-oxoethyl]cyclohexyl}phenyl)-7,8-dihydropyrimido[5,4-*f*][1,4]oxazepin-5(6H)-one (38)

LCMS (ESI) *m/z*: 452.5 (M+H).

5.1.33. 6-[4-(1-Acetyl)piperidin-4-yl]phenyl]-4-amino-7,8-dihydropyrimido[5,4-*f*][1,4]oxazepin-5(6H)-one (39)

A solution of 4-amino-6-(4-piperidin-4-ylphenyl)-7,8-dihydropyrimido[5,4-*f*][1,4]oxazepin-5(6H)-one (prepared in analogy to **1**²¹, starting with commercially-available *tert*-butyl 4-(4-chlorophenyl)piperidine-1-carboxylate, 17 mg, 0.05 mmol), (2-(7-aza-1*H*-benzotriazole-1-yl)-1,1,3,3-tetramethyluronium hexafluorophosphate) (38 mg, 0.1 mmol), triethylamine (20 mg, 0.2 mmol) and acetic acid (12 mg, 0.1 mmol) were stirred at ambient temperature for 17 h. Solvents were removed in vacuo and the residue purified by reverse phase chromatography to afford the title compound as white solid, 11 mg. LCMS (ESI) *m/z*: 382.1 (M+H).

The following compounds were made in analogy to **39**.

5.1.34. 4-Amino-6-[4-(1-isobutryl)piperidin-4-yl]phenyl]-7,8-dihydropyrimido[5,4-*f*][1,4]oxazepin-5(6H)-one (40)

LCMS (ESI) *m/z*: 410.2 (M+H).

5.1.35. 4-Amino-6-[4-[1-(ethoxyacetyl)piperidin-4-yl]phenyl]-7,8-dihydropyrimido[5,4-*f*][1,4]oxazepin-5(6H)-one (41)

LCMS (ESI) *m/z*: 426.1 (M+H).

5.1.36. 4-Amino-6-[4-[1-(cyclohexylcarbonyl)piperidin-4-yl]phenyl]-7,8-dihydropyrimido[5,4-*f*][1,4]oxazepin-5(6H)-one (42)

LCMS (ESI) *m/z*: 450.2 (M+H).

5.1.37. 4-Amino-6-[4-[1-(tetrahydro-2*H*-pyran-4-ylcarbonyl)piperidin-4-yl]phenyl]-7,8-dihydropyrimido[5,4-*f*][1,4]oxazepin-5(6H)-one (43)

LCMS (ESI) *m/z*: 452.1 (M+H).

5.1.38. 4-Amino-6-(4-[1-(*cis*-4-hydroxycyclohexyl)carbonyl]piperidin-4-yl)phenyl)-7,8-dihydropyrimido[5,4-*f*][1,4]oxazepin-5(6H)-one (44)

LCMS (ESI) *m/z*: 466.2 (M+H).

5.1.39. 4-Amino-6-[4-[1-(1,2,5-oxadiazol-3-ylcarbonyl)piperidin-4-yl]phenyl]-7,8-dihydropyrimido[5,4-*f*][1,4]oxazepin-5(6H)-one (45)

LCMS (ESI) *m/z*: 436.1 (M+H).

5.1.40. 4-Amino-6-[4-(1-benzoylpiperidin-4-yl)phenyl]-7,8-dihydropyrimido[5,4-*f*][1,4]oxazepin-5(6H)-one (46)

LCMS (ESI) *m/z*: 444.1 (M+H).

5.1.41. 4-Amino-6-[4-[1-(isoxazol-5-ylcarbonyl)piperidin-4-yl]phenyl]-7,8-dihydropyrimido[5,4-*f*][1,4]oxazepin-5(6H)-one (47)

LCMS (ESI) *m/z*: 435.1 (M+H).

5.1.42. 4-Amino-6-[4-[1-(isoxazol-3-ylcarbonyl)piperidin-4-yl]phenyl]-7,8-dihydropyrimido[5,4-*f*][1,4]oxazepin-5(6H)-one (48)

LCMS (ESI) *m/z*: 435.1 (M+H).

5.1.43. {*trans*-4-[4-(4-Amino-5-oxo-7,8-dihydropyrimido[5,4-*f*][1,4]oxazepin-6(5*H*)-yl)phenyl]cyclohexyl}acetoneitrile (49)

To a stirred solution of **29** (45 mg, 0.11 mmol) in tetrahydrofuran (1 mL) were added oxalyl chloride (0.05 mL, 0.6 mmol) and dimethylformamide (0.002 mL). After 2 h, saturated aqueous sodium bicarbonate was added and the mixture was diluted with ethyl acetate, washed with water, dried over sodium sulfate and concentrated in vacuo to afford the title compound as a light-yellow colored solid, 34 mg. ¹H NMR (400 MHz, DMSO-*d*₆): δ 8.17 (s, 1H), 7.63 (br s, 2H) 7.22 (m, 4H), 4.57 (m, 2H), 3.90 (m, 2H), 2.43 (m, 3H), 1.78 (m, 4H), 1.63 (m, 1H), 1.43 (m, 2H), 1.08 (m, 2H). LCMS (ESI) *m/z*: 378.3 (M+H).

5.1.44. 4-Amino-6-[4-{*trans*-4-(2-hydroxy-2-methylpropyl)cyclohexyl}phenyl]-7,8-dihydropyrimido[5,4-*f*][1,4]oxazepin-5(6H)-one (50)

To an ice cooled solution of **28** (40 mg, 0.10 mmol) was added methyl magnesium bromide (1.4 M in toluene, 0.83 mL, 1.16 mmol), the cooling bath was allowed to expire and the reaction mixture was stirred for 24 h. The reaction was partitioned between water and ethyl acetate, the organic phase dried over sodium sulfate and concentrated in vacuo. Chromatography on silica gel (4 g, 1–5% methanol/dichloromethane) afforded the title compound as a white solid, 10 mg. ¹H NMR (400 MHz, chloroform-*d*) δ 8.25 (s, 1H) 8.15 (br s, 1H) 7.22–7.30 (m, 2H) 7.12–7.19 (m, 2H) 5.71 (br s, 1H) 4.63–4.69 (m, 2H) 3.94–4.03 (m, 2H) 2.41–2.53 (m, 1H) 1.82–1.98 (m, 4H) 1.38–1.56 (m, 5H) 1.04–1.28 (m, 8H). LCMS (ESI) *m/z*: 411.4 (M+H).

5.1.45. 4-Amino-6-[4-{*trans*-4-(2-amino-2-methylpropyl)cyclohexyl}phenyl]-7,8-dihydropyrimido[5,4-*f*][1,4]oxazepin-5(6H)-one (51)

To a stirred solution of **50** (100 mg, 0.24 mmol) and trimethylsilylazide (42 mg, 0.37 mmol) was added boron trifluoride etherate (54 mg, 0.37 mmol) dropwise. After 30 h the reaction mixture was partitioned between ethyl acetate and saturated aqueous sodium bicarbonate. The organic layer was separated, dried over sodium sulfate to afford a white solid (106 mg), which was taken onto the next step without further purification.

The material prepared in the previous step was dissolved in ethyl acetate (10 mL)/ethanol (10 mL), 10% palladium-on-carbon (25 mg) was added and the slurry was shaken under an atmosphere of hydrogen gas (50 psi) for 20 h. The reaction mixture was filtered through a pad of Celite, washing with ethyl acetate and the combined filtrates were concentrated in vacuo. Chromatography on silica gel utilizing a gradient of 3–10% of 10% ammonium hydroxide in methanol/dichloromethane afforded the title compound as a white solid, 21 mg. ¹H NMR (400 MHz, methanol-*d*₄) δ 1.14 (s, 6H) 1.16–1.30 (m, 3H) 1.36 (d, *J* = 4.98 Hz, 2H)

1.40–1.62 (m, 3H) 1.88 (dd, $J = 23.06, 12.25$ Hz, 3H) 2.43–2.57 (m, 1H) 3.94–4.04 (m, 2H) 4.61–4.72 (m, 2H) 7.17–7.26 (m, 2H) 7.26–7.33 (m, 2H) 8.14 (s, 1H). LCMS (ESI) m/z : 410.0 (M+H).

5.1.46. 4-Amino-6-(4-{*trans*-4-[(3-methyl-1,2,4-oxadiazol-5-yl)methyl]cyclohexyl}phenyl)-7,8-dihydropyrimido[5,4-*f*][1,4]oxazepin-5(6H)-one (52)

To an ice cooled, stirred mixture of **1** (75 mg, 0.19 mmol) in 1,2-dichloroethane (0.63 mL) was added oxalyl chloride (0.165 mL, 1.89 mmol) and the resulting thick slurry was stirred at room temperature for 2 h. The mixture was concentrated in vacuo, azeotroped with toluene and the resulting solids dissolved in *p*-dioxane (1.5 mL), *N*-hydroxyacetamide (140 mg, 1.9 mmol) added and the mixture stirred at room temperature overnight. The reaction mixture was concentrated in vacuo and chromatographed on silica gel (12 g column, 5–10% methanol/dichloromethane over 30 min) to afford **68** as a white solid, 86 mg.

To a stirred solution of **68** (37 mg, 0.082 mmol) in dimethylformamide (1.0 mL) was heated under microwave conditions at 120 °C for 5 h. The reaction mixture was concentrated in vacuo and chromatographed on silica gel (12 g column, 2.5–10% methanol/dichloromethane over 30 min) to afford the title compound as a white solid, 23 mg. ¹H NMR (400 MHz, chloroform-*d*) δ 8.24 (s, 1H) 8.12 (br s, 1H) 7.20–7.28 (m, 2H) 7.11–7.19 (m, 2H) 5.67 (br s, 1H) 4.59–4.70 (m, 2H) 3.91–4.01 (m, 2H) 2.76 (d, 2H) 2.43–2.56 (m, 1H) 2.35 (s, 3H) 1.78–1.99 (m, 5H) 1.38–1.56 (m, 2H) 1.13–1.29 (m, 2H). LCMS (ESI) m/z : 435.1 (M+H).

5.1.47. 4-Amino-6-(4-{*trans*-4-[(5-methyl-1,3,4-oxadiazol-2-yl)methyl]cyclohexyl}phenyl)-7,8-dihydropyrimido[5,4-*f*][1,4]oxazepin-5(6H)-one (53)

To an ice cooled, stirred mixture of **1** (100 mg, 0.252 mmol) in 1,2-dichloroethane (0.84 mL) was added oxalyl chloride (0.221 mL, 2.52 mmol) and the resulting thick slurry was stirred at room temperature for 2 h. The mixture was concentrated in vacuo, azeotroped with toluene and the resulting solids dissolved in *p*-dioxane (1.5 mL), acetic hydrazide (192 mg, 2.52 mmol) added and the mixture stirred at room temperature for 96 h. The reaction mixture was partitioned between dichloromethane and saturated aqueous sodium bicarbonate. The insoluble solids were filtered, washed with water and dried in vacuo to afford **69** as a white solid, 83 mg.

To a stirred solution of triphenylphosphine (23 mg, 0.021 mmol), iodine (21 mg, 0.084 mmol) and triethylamine (18 mg, 0.176 mmol) was added **69** (20 mg, 0.044) and the resulting mixture was stirred at room temperature for 3.5 h. The reaction mixture was concentrated in vacuo and chromatographed via prep HPLC (C18 column, 20–50% acetonitrile/water, 10 mL/min) to afford the title compound as a white solid, 6 mg. ¹H NMR (400 MHz, chloroform-*d*) δ 8.24 (s, 1H) 8.15 (br s, 1H) 7.20–7.30 (m, 2H) 7.11–7.19 (m, 2H) 5.72 (br s, 1H) 4.61–4.68 (m, 2H) 3.93–4.02 (m, 2H) 2.68–2.76 (m, 2H) 2.41–2.55 (m, 4H) 1.80–1.95 (m, 5H) 1.37–1.54 (m, 2H) 1.13–1.28 (m, 2H). LCMS (ESI) m/z : 435.3 (M+H).

5.1.48. 4-Amino-6-(4-{*trans*-4-[(5-methyl-1,3,4-thiadiazol-2-yl)methyl]cyclohexyl}phenyl)-7,8-dihydropyrimido[5,4-*f*][1,4]oxazepin-5(6H)-one (54)

A solution of **69** (26 mg, 0.057 mmol) and Lawesson's reagent (14 mg, 0.034 mmol) in 1:1 *p*-dioxane:tetrahydrofuran (0.8 mL) was heated in a sealed tube at 120 °C for 18 h. The reaction was cooled, concentrated and chromatographed via prep HPLC (C18 column, 20–50% acetonitrile/water, 10 mL/min) to afford the title compound as a white solid, 2.5 mg. ¹H NMR (400 MHz, methanol-*d*₄) δ 8.12 (s, 1H) 7.26–7.32 (m, 2H) 7.19–7.25 (m, 2H) 4.63–4.69 (m, 2H) 3.96–4.02 (m, 2H) 2.97–3.01 (m, 2H) 2.70 (s, 3H) 2.48–2.58 (m, 1H) 1.83–1.92 (m, 5H) 1.42–1.57 (m, 2H) 1.18–1.30 (m, 2H). LCMS (ESI) m/z : 451.1 (M+H).

5.1.49. 4-Amino-6-(4-{*trans*-4-[(5-methyl-4H-1,2,4-triazol-3-yl)methyl]cyclohexyl}phenyl)-7,8-dihydropyrimido[5,4-*f*][1,4]oxazepin-5(6H)-one (55)

To an ice cooled, stirred mixture of **1** (50 mg, 0.13 mmol) in 1,2-dichloroethane (0.42 mL) was added oxalyl chloride (0.11 mL, 1.26 mmol) and the resulting thick slurry was stirred at room temperature for 2 h. The mixture was concentrated in vacuo, azeotroped with toluene and the resulting solids dissolved in tetrahydrofuran (3 mL). Acetamidrazone hydrochloride (41 mg, 0.38 mmol) and triethylamine (39 mg, 0.38 mmol) were added and the mixture was stirred for 3 h. The reaction was concentrated in vacuo and purified via medium pressure silica gel chromatography (10 g column, 15 mL/min, 5–10% methanol/dichloromethane) to afford **70** as a white solid, 18 mg.

A stirred solution of **70** (18 mg, 0.04 mmol) in DMF (1 mL) was heated at 140 °C for 4 h, concentrated in vacuo and purified via medium pressure silica gel chromatography (10 g column, 15 mL/min, 5–10% methanol/dichloromethane) to afford the title compound as a yellow solid, 0.5 mg. ¹H NMR (400 MHz, chloroform-*d*) δ 8.25 (s, 1H), 7.23–7.28 (m, 2H), 7.12–7.18 (m, 2H), 4.65 (dd, $J = 4.98, 3.61$ Hz, 2H), 3.90–4.02 (m, 2H), 2.34–2.42 (m, 6H), 2.12 (d, $J = 6.83$ Hz, 1H), 1.90 (br s, 5H), 1.40–1.60 (m, 3H). LCMS (ESI) m/z : 432 (M+H).

5.1.50. 4-Amino-6-(4-{*trans*-4-[(4,5-dimethyl-4H-1,2,4-triazol-3-yl)methyl]cyclohexyl}phenyl)-7,8-dihydropyrimido[5,4-*f*][1,4]oxazepin-5(6H)-one (56)

To an ice cooled, stirred mixture of **1** (50 mg, 0.13 mmol) in 1,2-dichloroethane (0.42 mL) was added oxalyl chloride (0.11 mL, 1.26 mmol) and the resulting thick slurry was stirred at room temperature for 2 h. The mixture was concentrated in vacuo, azeotroped with toluene and the resulting solids dissolved in 2 M methylamine in tetrahydrofuran (0.63 mL, 1.26 mmol) and stirred for 24 h. The solids were filtered, washed with ethyl ether and dried in vacuo to afford 2-{4-[4-(4-amino-5-oxo-7,8-dihydro-5H-9-oxa-1,3,6-triaza-benzocyclohepten-6-yl)-phenyl]-cyclohexyl}-*N*-methylacetamide as a white solid, 50 mg.

A solution of 2-{4-[4-(4-amino-5-oxo-7,8-dihydro-5H-9-oxa-1,3,6-triaza-benzocyclohepten-6-yl)-phenyl]-cyclohexyl}-*N*-methylacetamide (35 mg, 0.085 mmol) and Lawesson's reagent (21 mg, 0.051 mmol) in tetrahydrofuran (0.57 mL) was heated at reflux for 3 h. The reaction was cooled, concentrated in vacuo and chromatographed on silica gel (4 g, 2–8% methanol/dichloromethane, 30 min) to afford **71** as a yellow solid, 11 mg.

A stirred slurry of **71** (11 mg, 0.026 mmol), mercury oxide (6.4 mg, 0.029 mmol) and acetic hydrazide (4 mg, 0.052 mmol) in tetrahydrofuran was stirred at room temperature for 16 h and then heated at 80 °C under microwave conditions. The reaction mixture was filtered through Celite®, washing with methanol and then chromatographed via prep HPLC (C18, 20–50% acetonitrile/water, 10 mL/min) to afford the title compound as a white solid, 4 mg. ¹H NMR (400 MHz, chloroform-*d*) δ 8.22 (s, 1H) 8.16 (br s, 1H) 7.24 (d, 2H) 7.14 (d, 2H) 6.02 (br s, 1H) 4.61–4.68 (m, 2H) 3.94–4.01 (m, 2H) 3.46 (s, 3H) 2.65 (d, 2H) 2.45–2.54 (m, 1H) 2.41 (s, 3H) 1.77–1.94 (m, 5H) 1.36–1.51 (m, 2H) 1.13–1.29 (m, 2H). LCMS (ESI) m/z : 448.2 (M+H).

5.1.51. 4-Amino-6-(4-{*trans*-4-[2-(3-methyl-1,2,4-oxadiazol-5-yl)ethyl]cyclohexyl}phenyl)-7,8-dihydropyrimido[5,4-*f*][1,4]oxazepin-5(6H)-one (57)

Prepared in analogy to **52**, employing **25** as the starting material. ¹H NMR (400 MHz, chloroform-*d*) δ 8.23 (s, 1H), 8.21–8.02 (m, 1H), 7.27–7.09 (m, 4H), 5.80–5.55 (m, 1H), 4.68–4.57 (m, 2H), 4.00–3.91 (m, 2H), 2.90–2.79 (m, 2H), 2.52–2.41 (m, 1H), 2.37–2.31 (m, 3H), 1.8 (d, $J = 12.30$ Hz, 4H), 1.77–1.61 (m, 2H), 1.49–1.29 (m, 3H), 1.16–1.01 (m, 2H). LCMS (ESI) m/z : 449.3 (M+H).

5.2. Molecular modeling

The conformational analysis was performed using OPLS_2005 force field.^{31,32}

5.3. Biology

5.3.1. Enzyme and whole-cell assays

Experimental procedures for DGAT-1 enzymatic and HT-29 whole cell assays, as well as the triglyceride tolerance test in rats can be found in the supporting information section of Ref. 21.

5.3.2. 14-Day efficacy study in db/db mice

Male db/db mice (Charles River, Wilmington, MA) were bled, randomized for body weight and housed four per cage in hanging wire cages (4 per/cage/dose) at 21 ± 2 °C with a 12:12 h light:dark cycle, fed a pelleted high fat Western diet (Research Diets, New Brunswick, NJ) and had ad libitum access to water. All procedures were approved by and conducted in accordance with Institutional Animal Care and Use Committee guidelines and regulations. At 4:00 pm of day 0, animals were dosed with 1, 3 or 15 mg/kg of 52 or 0.5% methylcellulose vehicle ($n = 8$). Food, water and body weight measurements were collected daily at 4:00 pm immediately prior to dosing. Fed plasma triglyceride and non-esterified free fatty acid were collected from orbital sinus bleeds 16 h post dose on days 0, 7 and 14. Liver biopsies were collected on day 14, 16 h after final dose. Satellite PK groups ($n = 4$) were dosed utilizing the protocols described above.

6. Author contributions

The manuscript was written through contributions of all authors. All authors have reviewed the final version of the manuscript

Acknowledgement

The authors would like to thank Philip Carpino for editorial comments on this manuscript.

References and notes

- McGarry, J. D. *Diabetes* **2002**, *51*, 7.
- Alberti, K. G.; Zimmet, P.; Shaw, J. *Lancet* **2005**, *366*, 1059.
- Stein, D. T.; Dobbins, R.; Szczepaniak, L.; Malloy, C.; McGarry, J. D. *Diabetes* **1997**, *46*, 23A.
- Szczepaniak, L. S.; Babcock, E. E.; Schick, F.; Dobbins, R. L.; Garg, A.; Burns, D. K.; McGarry, J. D. *Am. J. Physiol.* **1999**, *276*, E977.
- Huang-Doran, I.; Sleigh, A.; Rochford, J. J.; O'Rahilly, S.; Savage, D. B. *J. Endocrinol.* **2010**, *207*, 245.
- Unger, R. H.; Zhou, Y.-T.; Orci, L. *Proc. Natl. Acad. Sci. U.S.A.* **1999**, *96*, 2327.
- Shimonura, I.; Hammer, R. E.; Ikemoto, S.; Brown, M. S.; Goldstein, J. L. *Nature* **1999**, *401*, 73.
- Coleman, R. A.; Lee, D. P. *Prog. Lipid Synth.* **2004**, *43*, 134.
- Koltun, D. O.; Zablocki, J. Enzymatic targets in the triglyceride synthesis pathway. In *Annual Reports in Medicinal Chemistry*, volume 45; Macor, J. E., Ed.; Academic Press, New York, 2010; pp 109–122.
- Kayden, H. J.; Senior, J. R.; Mattson, F. H. *J. Clin. Invest.* **1967**, *46*, 1695.
- Kennedy, E. P. *Annu. Rev. Biochem.* **1957**, *26*, 119.
- Cases, S.; Smith, S. J.; Zheng, Y. W.; Myer, H. M.; Lear, S. R.; Sande, E.; Novak, S.; Collins, C.; Welch, C. B.; Lusic, A. J.; Erickson, S. K.; Farese, R. V., Jr. *Proc. Natl. Acad. Sci. U.S.A.* **1998**, *95*, 13018.
- Oelkers, P.; Behari, A.; Cromley, D.; Billheimer, J. T.; Sturley, S. L. *J. Biol. Chem.* **1998**, *273*, 26765.
- Cases, S.; Stone, S. J.; Zhou, P.; Yen, E.; Tow, B.; Lardizabal, K. D.; Voelker, T.; Farese, R. V., Jr. *J. Biol. Chem.* **2001**, *276*, 38870.
- Smith, S. J.; Cases, S.; Jensen, D. R.; Chen, H. C.; Sande, E.; Tow, B.; Sanan, D. A.; Raber, J.; Eckel, R. H.; Farese, R. V. *Nat. Genet.* **2000**, *25*, 87.
- Chen, H. C.; Smith, S. J.; Ladha, Z.; Jensen, D. R.; Ferreira, L. D.; Pulawa, L. K.; McGuire, J. G.; Pitas, R. E.; Eckel, R. H.; Farese, R. V. *J. Clin. Invest.* **2002**, *109*, 1049.
- Chen, H. C.; Jensen, D. R.; Myers, H. M.; Eckel, R. H.; Farese, R. V. *J. Clin. Invest.* **2003**, *111*, 1715.
- Dow, R. L. Acyl-CoA: Diacylglycerol Acyltransferase-1 Inhibition as an Approach to the Treatment of Type 2 Diabetes. In *New Therapeutic Strategies for Type 2 Diabetes*; Jones, R. M., Ed.; RSC Publishing: Cambridge, UK, 2012; pp 215–248.
- King, A. J.; Judd, A. S.; Souers, A. J. *Expert Opin. Ther. Patents* **2010**, *20*, 19.
- Birch, A. M.; Buckett, L. K.; Turnbull, A. V. *Curr. Opin. Drug Disc. Dev.* **2010**, *13*, 489.
- Dow, R. L. Li, J.-C.; Pence, M. P.; Gibbs, E. M.; LaPerle, J. L.; Litchfield, J.; Piotrowski, D. W.; Munchhof, M. J.; Manion, T. B.; Zavadski, W. J.; Walker, G. S.; McPherson, R. K.; Tapley, S.; Sugarman, E.; Guzman-Perez, A.; DaSilva-Jardine, P. *ACS Med. Chem. Lett.* **2011**, *2*, 407.
- Fox, B. M.; Furukawa, N. H.; Hao, X.; Lio, K.; Inaba, T.; Jackson, S. M.; Kayser, F.; Labelle, M.; Kexue, M.; Matsui, T.; McMinn, D. L.; Ogawa, N.; Rubenstein, S. M.; Sagawa, S.; Sugimoto, K.; Suzuki, M.; Tanaka, M.; Ye, G.; Yoshida, A.; Zhang, J. A. Preparation of fused bicyclic nitrogen-containing heterocycles, useful in the treatment or prevention of metabolic and cell proliferative diseases. WO 2004/047756A2, Chem. Abstr. 141:38623.
- Calculated passive permeability of 5×10^{-6} cm/s. The calculated passive permeability is based on a Pfizer training set of 126,024 measured passive permeabilities.
- Dow, R. L.; Carpino, P. A.; Hadcock, J. R.; Black, S. C.; Iredale, P. A.; DaSilva-Jardine, P.; Schneider, S. R.; Paight, E. S.; Griffith, D. A.; Scott, D. O.; O'Connor, R. E.; Nduaka, C. I. *J. Med. Chem.* **2009**, *52*, 2652.
- Brabec, M. J. Aldehydes and acetals. In *Patty's Industrial Hygiene and Toxicology*, Clayton, G. D.; Clayton, F. E., Eds.; John Wiley & Sons, Inc: New York, 1993; vol. IIB, 2629.
- Hopkins, A. L.; Groom, C. R.; Alex, A. *Drug Discovery Today* **2004**, *9*, 430.
- Di, L.; Whitney-Pickett, C.; Umland, J. P.; Zhang, H.; Zhang, X.; Gebhard, D. F.; Lai, Y.; Federico, J. J., III; Davidson, R. F.; Smith, R.; Reyner, E. L.; Lee, C.; Feng, B.; Rotter, C.; Varma, M. V.; Kempshall, S.; Fenner, K.; El-Kattan, A. F.; Liston, T. E.; Troutman, M. D. *J. Pharm. Sci.* **2011**, *100*, 4974.
- Meanwell, N. A. *J. Med. Chem.* **2011**, *54*, 2529.
- Villaneuva, C. J.; Monetti, M.; Shih, M.; Zhou, P.; Watkins, S. M.; Bhanot, S.; Farese, R. V., Jr. *Hepatology* **2009**, *50*, 434.
- Kusunoki, M.; Tsutsumi, K.; Hara, T.; Ogawa, H.; Nakamura, T.; Sakakibara, F.; Fukuzawa, Y.; Suga, T.; Kakumu, S.; Nakaya, Y. *Metabolism* **2002**, *51*, 792.
- Jorgensen, W. L.; Maxwell, D. S.; Tirado-Rives, J. *J. Am. Chem. Soc.* **1996**, *118*, 11225.
- Kaminski, G. A.; Friesner, R. A.; Tirado-Rives, J.; Jorgensen, W. J. *J. Phys. Chem. B* **2001**, *105*, 6474.